Technical Report C84-02
August 1984

GLOBAL SEISMIC NETWORK ASSESSMENT FOR TELESEISMIC DETECTION OF UNDERGROUND NUCLEAR EXPLOSIONS

Hans-Peter Harjes

Sponsored by:
DEFENSE ADVANCED RESEARCH PROJECTS AGENCY
Monitored by:
Defense Supply Service – Washington
Under Contract No. MDA 903-84-C-0020

Science Applications International Corp.
1735 Jefferson Davis Highway, Suite 907
Arlington, VA 22202

This research was accomplished during 1984 while the author was a visiting scientist at the Center for Seismic Studies. Partial support was provided by the Defense Advanced Research Projects Agency through Science Applications International Corporation under Contract No. MDA903-84-C-0020, ARPA Order 4882.

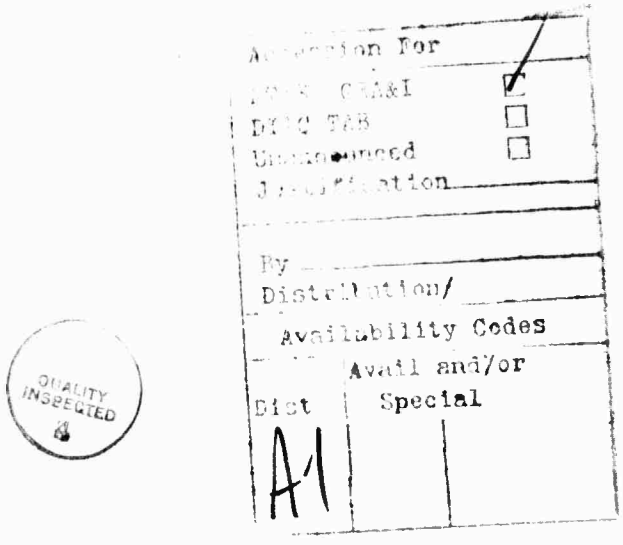

Global Seismic Network Assessment for Teleseismic Detection of Underground Nuclear Explosions

Hans-Peter Harjes
Ruhr-University Bochum, F. R. Germany

ABSTRACT

The detection capability of a global seismic network is examined on the basis of a probabilistic model: Given the location of seismograph stations with known background noise level, a worldwide grid of epicenters, and amplitude-distance attenuation curves, the detection capability is expressed by the magnitude corresponding to a fixed probability that a specified minimum number of stations detect an event.

A globally distributed network of 50 stations is selected and multiwave detection criteria are applied which take variation of attenuation for different wave types into consideration. The extension of amplitude-attenuation curves to include core phases is investigated and effects of regional attenuation are studied. Depending on the detection criterion and attenuation curve, magnitude thresholds of a 50-station network can significantly vary.

The largest influence, however, results from changes in station noise data. Reliable estimates of noise statistics can only be derived from continuous measurements in connection with routine event readings. An indirect method to calculate noise parameters is demonstrated by using station detection thresholds. After estimation of noise statistics from station reportings to the International Seismological Centre (ISC) for 1980, predicted magnitude detection thresholds and empirical values are in good agreement.

Magnitude thresholds for teleseismic detection range between $4.0 \leqslant m_b \leqslant 4.5$ in the northern hemisphere and between $4.5 \leqslant m_b \leqslant 4.9$ in the southern hemisphere. Model calculations show that these thresholds can be lowered at least half a magnitude unit after current seismological instrumentation and observatory practice have been improved.

I. Introduction

> "Although seismological capacity for identifying underground nuclear explosions may now be secondary to the political will of parties engaged in Comprehensive Test Ban negotiations it is still important to present the clearest possible evaluation of the role seismology might play should a Comprehensive Test Ban become reality."

This quotation from a 12 year old paper (Marshall and Basham, 1972) is still an adequate description of the general purpose of studies on seismic verification of nuclear test ban treaties. In a more specific sense we want to assess the detection threshold of a network of modern seismic stations. Detection thresholds will be given in terms of magnitude. Therefore, thresholds described herein apply to both shallow earthquakes and underground explosions without regard to source type. The important questions of source identification and yield estimation are not addressed in this paper. Previous detection studies include the SIPRI-report (Davies, 1968), an analysis initiated by the United Nations (Basham and Witham, 1970), and a report of a group of seismologists to the Conference on Disarmament in Geneva (CCD/558, 1978). All of these assessments present conceptually similar schemes whereby worldwide existing seismological facilities are applied to a straightforward statistical estimation model: Given a globally distributed network of seismograph stations with known background noise level, a set of epicenter locations, and standard amplitude-distance attenuation curves for seismic waves, the detection capability is expressed by the magnitude corresponding to a fixed probability that a specified minimum number of stations detect an event.

A second group of papers (Kelly and Lacoss, 1969), (Report US/GSE/7, 1980) describe a different approach to examine the detection capability of a seismic network by including average worldwide seismicity. Using known earthquake recurrence rates a synthetic list of events is produced as a reasonable approximation to those actually observed in a specific time interval. Keeping station parameters unchanged, this method allows an independent check on the results of studies of the first kind.

Finally, a third procedure starts from real data collected during special experiments (Lacoss et al., 1974) or published in bulletins by international agencies (e.g., International Seismological Centre (ISC) in Newbury, UK) and estimates detection thresholds with the use of gaussian or maximum-likelihood techniques (Ringdal et al., 1977), (Ringdal, 1984).

Detection capabilities of seismic networks differ substantially as a result of these various approaches, in general the detection threshold increases in the order of the described procedures. Some reasons for these differences are obviously due to the difference between operational station performance used in the last approach and the idealized assumptions based on pure noise statistics which are input to the process mentioned first. Smaller discrepances simply reflect the difficulty in making this type of estimate and should be kept in mind in judging on the accuracy of the results.

This report has three main purposes:

(i) To examine recently published approaches to network detection capability estimation by using multiwave detection criteria. A computer coded version of this procedure (Ciervo et al., 1983) was made available at the Center for Seismic Studies (CSS) in Arlington, VA. This code, called "Seismic Network Assessment Program for Detection (SNAPD)," not only models the propagation of p-waves which were employed in previous programs (Wirth, 1977) but takes all relevant seismic phases into account and calculates wave attenuation and travel time as a function of regional media characteristics and event type.

(ii) To study the influence of geophysical input parameters on the outcome. These parameters include especially the amplitude attenuation curves at teleseismic distances and also the extension to core phases. Variations of attenuation in tectonic and stable areas at regional distances are of special importance for detailed epicenter-station configurations. Special attention will be given to amplitude attenuation curves derived from seismograms of underground nuclear explosions; otherwise earthquake data are included using shallow events.

(iii) To reconsider the results with most recent station data which became available after installation of a large number of digitally recording seismographs. Some conclusions can already been drawn from the data reported to the ISC for 1980. These data are used to compare maximum-likelihood detection estimates (Ringdal, 1984) with results from the new network detection code.

II. Analysis of Network Detection Probabilities

The statistical model and basic computational procedures are described in this section. The model includes various parameters to be known at the beginning. The most important are:

- Seismic station locations and their noise statistics (mean and variance)
- Amplitude distance relations for several phases (besides p-waves and R-waves the prominent regional phases pg and lg are used)
- Signal-to-noise ratio required for detection.

The procedure is then to do the following:

- Select a source location and compute detection probabilities for each station as a function of event magnitude.
- Find the lowest magnitude for which there is a defined probability to meet the specific detection criterion. (The most frequent criterion for global detection studies asks for a 90 per cent probability of detecting p-waves by at least four stations.)

First, a single station is considered and the probability that it detects a certain wave is derived. Then the multiwave detection probability and the network capability are defined. We closely follow the notation by Ciervo et al., (1983). Further details can be found in Wirth, (1977) and Elvers, (1980).

p_{ijk} denotes the probability that wave k propagated from epicenter j will be observed at station i. It is given by

$$p_{ijk}=R_i\Phi\left[\frac{\log A_{ijk}^{(\alpha)}-(\mu_{ik}+\log r_{ik})}{\sqrt{\sigma_{n_{ik}}^2+\sigma_{s_{ik}}^2+\sigma_{bk}^2}}\right] \tag{1}$$

where

$$\Phi(x)\equiv\int_{-\infty}^{x} e^{\frac{-y^2}{2}}\frac{dy}{\sqrt{2\pi}} \tag{2}$$

is the normal cumulative probability function.

In Equation (1) signal and noise are assumed to be log normally distributed and the log of the noise amplitude has expectation μ_n and variance σ_n^2 and the log of the signal variance is σ_s^2. σ_{bk}^2 defines the additional variance of the log signal amplitude for wave k, given an m_b value; hence $\sigma_{bk}\equiv 0$ if k denotes the p-wave. A station i is supposed to detect wave k provided that the ratio of signal to noise is at least r_{ik}.

Given an event at epicenter j of magnitude m_b and distance Δ_{ij} from station i, the amplitude of wave k at that station is calculated as

$$\log A_{ijk}^{(\alpha)}=m_{k_j}+b_k^{(\alpha)}(\Delta_{ij})+c_k^{(\alpha)}\log(\Delta_{ij})+\epsilon_{ijk} \tag{3}$$

for both stable ($\alpha=S$) and tectonic ($\alpha=T$) media. For waves other than conventionally used p-phase m_b has to be converted into an adequate magnitude m_k given the respective regression formula

$$m_{k_j}=[KE]_k+[KM]_k m_b \tag{4}$$

The b_k and c_k in Equation (3) are attenuation table entries, and ϵ_{ijk} is the epicenter-station calibration term for wave k.

If wave k does not require regional attenuation or if $\Delta > 25deg$ then $\log A_{ijk}$ is computed directly from (3) using a stable medium attenuation table. Otherwise for regional distances ($\Delta \leqslant 25deg$)

$$\log A_{ijk} = (1-w_{ij}) log A_{ijk}^{(S)} + w_{ij} \log A_{ijk}^{(T)} \tag{5}$$

where w_{ij} is the regional path weight; i.e., the ratio of the length of the wave path in tectonic media to the total great-circle path length Δ_{ij}. Especially if the epicentral path is assumed to have passed a region that severely attenuates lg-waves, then $\log A_{ij(lg)} = -\infty$.

If the attenuation table entries are δ_k, b_k, c_k,
then for $\delta_{k-1} < \Delta_{ij} < \delta_k$

$$b_{\Delta_{ij}} \equiv b_k \text{ and } c_{\Delta_{ij}} \equiv c_k \tag{6}$$

except that if $c_k = 0$, linear interpolation is used for b:

$$b_{\Delta_{ij}} = b_k - (\delta_k - \Delta_{ij})[b_k - b_{k-1}]/(\delta_k - \delta_{k-1}) \tag{7}$$

The station's probability of detection p_{ijk}, given by Equation (1) is influenced by the reliability R_i of its operation. p_{ijk} includes therefore, a factor $R_i, 0 < R_i \leqslant 1$. R_i is of course dependent on a number of local circumstances which are not well known. Usually we set $R_i = 1$, assuming perfect operation.

Given the probability for a single station to detect an individual wave, we have to develop a procedure for multiwave network detection criteria that use combinations of dependent wave arrivals at individual stations. An essential feature in the development of the model is the assumption that a minimum of four phases (not more than two of which are recorded at the same station) are required for detection assessment. Although relaxations of this requirement are possible, they do not seem to be desirable with regard to later location procedures.

As an example we illustrate the detection criterion

$$(p_g \cap l_g)/2 \cup p/4 \tag{8}$$

which literally means that a network detection consists of at least a two-station detection of pg and lg regional waves or at least a four-station detection of p-waves. Expression (8) consists of two subcriteria:

$$\mathbf{D}^1 = (p_g \cap l_g)\ /2 \qquad \mathbf{D}^2 = p/4$$

which specify different wave combinations.

The detection criteria such as Equation (8) have to be decomposed and reduced to a set of canonical probabilities. Therefore, the logical expression (8) is transformed into an algebraic expression involving the marginal probabilities of independent subcriteria and the joint probabilities of dependent pairs of subcriteria. This transformation eliminates all logical "or" ($\bigcup$) among subcriteria by use of the elementary rule

$$prob\ [\mathbf{D}^1/n \bigcup \mathbf{D}^2/m] = prob[\mathbf{D}^1/n\ ] + prob[\mathbf{D}^2/m] \qquad (9)$$

$$- prob\ [\mathbf{D}^1/n \bigcap \mathbf{D}^2/m]$$

where, if $\mathbf{D}^1$ and $\mathbf{D}^2$ have no waves in common

$$prob\ [\mathbf{D}^1/n \bigcap \mathbf{D}^2/m\ ] = prob\ [\mathbf{D}^1/n\ ]\ prob\ [\mathbf{D}^2/m\ ] \qquad (10)$$

In case of Equation (10) independent calculations for each individual wave define the probability $prob[\mathbf{D}_{(n':N)}]$ that exactly n out of N stations detect wave combination $\mathbf{D}^1$. If, however, the detection subcriteria $\mathbf{D}^1$ and $\mathbf{D}^2$ have waves in common like

$$(l_g/2 \bigcap p/1) \bigcup p/4$$

then computation of the joint probability (10) does not split into independent probabilities.

Clearly, the probability $prob[\mathbf{D}^1/n]$ of at least n detecting stations follows as :

$$prob\ [\mathbf{D}^1/n\ ] = \sum_{n'=n}^{N} prob\ [\mathbf{D}^1_{(n':N)}\ ] \qquad (11)$$

Thus, we need only to compute the probability of exactly n' detecting stations.

In a concluding step a binary search is used to find the magnitude value that results in p_t, the threshold probability for network detection. Let m_i be a sequence of test magnitudes $m_{min} \leq m_i \leq m_{max}$ such that each m_i results in a network detection probability p_i. Initially $m_1 = m_{min}$. If $p_1 \geq p_t$, the search is terminated; otherwise $m_2 = m_{max}$ and if $p_2 \leq p_t$, the search is also terminated. Assuming $p_1 < p_t < p_2$

$$m_i = (m_{i-1} + m')/2 \quad i=1,2,3,..$$

where, if p_{i-1} is less than p_t, m' is the last test magnitude for which the corresponding network probability is greater than p_t, and vice versa.

The search is continued until $i=i^*$ is reached such that

$$|p_{i^*} - p_t| \leq \epsilon$$

corresponding to a threshold magnitude m_{i^*}.

III. Detection Capability of a Global Network

In selecting a network for detection of seismic events based upon existing seismograph stations, it is desirable to

- arrive at a relatively uniform geographical distribution of stations
- select stations with modern instrumentation and optimum detection capabilities.

With these criteria in mind a selection of relatively few stations is considerably more effective than using all (about 1000) stations that routinely report to one of the international data centers. In a previous report (CCD/558, 1978) a network of 50 stations has been composed which was judged to produce the best seismological results currently achievable for teleseismic detectior of seismic events.

These stations whose geographical distribution is shown in Figure 1 and whose coordinates and further parameters are given in Table 1 are used as a reference network in our study. The global station distribution is not as uniform as desirable having 36 stations in the northern hemisphere compared to 14 stations in the southern hemisphere or 31 stations in the eastern hemisphere compared to 19 in the western hemisphere, but it reflects to some extent the distribution of land masses on earth.

Mean value and standard deviation of logarithmic station noise which are used to calculate station detection probabilities from Equation (1) are also included in Table 1 (columns 4 and 5). Due to the quoted report (CCD/558, 1978) average noise levels were partly derived from published noise power spectra, partly estimated from magnification curves of seismographs. Because of lack of adequate measurements an adhoc procedure was used to estimate the variance of the station noise; those stations with higher noise level were also assigned greater variance.

As can be seen from Equation (1) it is the combined effect of variance in noise amplitude and signal amplitude which influences the station detection threshold; it decreases as the denominator in Equation (1) is increased provided that the detection probability is less than 0.5, and vice versa. For the network the detection threshold generally decreases when signal or noise variance is increased. For the 50 station network - introduced in Figure 1 and Table 1 - a constant value for the standard deviation of signal amplitude (0.2 in logarithmic units) was used. Test runs showed that doubling this parameter to 0.4 result in a very small difference of the network detection threshold (not exceeding 0.1 magnitude unit). Consequently, network capability is not very sensitive to this parameter.

There are two other input parameters to Equation (1) which are to be assumed in an adhoc manner: the reliability factor R describing grossly the station operation (up-time) is set in our calculations to 1.0. Earlier studies (Ringdal et al., 1977) have estimated this parameter to range from 0.8 to 1.0 for most of the stations selected for our network.

A minimum signal-to-noise ratio has to be chosen to detect seismic signals emerging from background noise. Throughout this study a s/n ratio (r_{ik} in Equation (1)) of 1.5 was chosen. The capability results are easily transformed to correspond to other s/n ratios, since this parameter occurs as a difference $(m-\log r_{ik})$ in Equation (1). Thus, a simple relationship exists between the chosen value of r_{ik} and the corresponding magnitude level. If r_{ik} is increased from 1.5 to 3.0, for example, the threshold will be increased by $(log3-\log 1.5)=0.3$ magnitude units.

a. Amplitude-Attenuation Curves at Teleseismic Distances: $25deg<\Delta<100deg$

Several investigations of amplitude attenuation with distance have been made since the pioneering work of Gutenberg and Richter, (1956). According to their paper we will summarize amplitude-distance relations from Equation (3) in the form

$$B\ (\Delta) = b\ (\Delta) + c \cdot \log\ (\Delta)$$

So we can interpret B-values in terms of magnitude units.

In Figure 2 the results of Evernden and Clark, (1970), Veith and Clawson, (1972) and NORSAR ( ) are compared to the Gutenberg and Richter curve. Whereas, Evernden and Clark as well as Veith and Clawson use mostly explosions and a station network of mainly LRSM-stations in the U.S., the NORSAR-curve is derived from observations of teleseismic events at a single array site.

All curves have been arbitrarily connected at regional distances to focus upon the differences in the teleseismic window. The principal difference between Veith-Clawson and NORSAR curves on one hand and

Gutenberg-Richter and Evernden-Clark curves on the other hand appears in the fact that the former smooth amplitude variations from mantle discontinuities, whereas the latter indicate several step-wise changes in amplitude as a function of distance. The difference between Veith-Clawson and NORSAR attenuation curves is nearly a constant 0.1 magnitude unit over the whole teleseismic range. This may result from the fact that the Veith-Clawson curve was corrected for surface focus events; in comparison, the NORSAR curve comprises measurements from shallow earthquakes. The obvious distinction between the curve of Gutenberg-Richter and Evernden-Clark appears in the far teleseismic portion where a difference of 0.3 magnitude units can be found. This is a consequence of the way Evernden and Clark have chosen to normalize their data.

Some of these differences can be seen in the network detection capability which is shown in Figures 3-6. Using a 15 deg epicenter grid the 90 per cent probability of at least four detecting stations was calculated. For the NORSAR attenuation function (Figure 3), which will be used as a reference curve in this study, the magnitude threshold is estimated to be from m_b 3.4 to 3.7 in Europe and Scandinavia, m_b 3.7 to 3.8 in North America, Asia, and Arctica, m_b 3.7 to 4.0 in Africa and most parts of South America, whereas we get values up to m_b=4.5 in the Pacific region. The slight difference between the eastern and western hemisphere (about 0.2 magnitude units) as well as the large difference of more than one magnitude unit between the northern and southern hemisphere mainly result from the station distribution of the network. The high station noise at the sites in the Pacific (New Zealand and Samoa) gives an additional contribution to the low detection capability in the southern hemisphere.

As expected from the preceding discussion of attenuation curves (Figure 2) detection thresholds for the network increase globally by 0.1 magnitude unit using the Veith-Clawson data. The Evernden-Clark curve has a remarkable effect in lowering the detection threshold in the southern hemisphere by about 0.3 magnitude units (Figure 5), again not unexpected from the shape of the attenuation curve which shows pronounced lower B-values at far teleseismic distances than any other attenuation curve in Figure 2. Finally, Gutenberg-Richter curve yields detection thresholds (Figure 6) very similar to Veith-Clawson curve (Figure 4).

We can conclude from these calculations that step-wise changes in the attenuation curve do not significantly effect the global detection capability of a 50-station network. Of course these discontinuities have remarkable focussing-defocussing effects for specific epicenter-station configurations, but these are smoothed and can not be resolved by global grids of 15 deg size. These peculiarities are better implemented by use of epicenter-station calibration factors expressed by ϵ_{ijk} in Equation (3).

For all computations we kept the probability level at 90 per cent. In changing this parameter one can significantly influence detection thresholds

(of course the seismological capability is not changed at all). At the 30 per cent probability level (Figure 7) we get 0.2 - 0.4 magnitude units lower thresholds compared to the commonly accepted 90 per cent probability level.

Another way of demonstrating this difference is to calculate the network detection probability for a fixed magnitude value. Figure 8 shows the global distribution of probabilities to detect a magnitude 4 event. Besides Antarctica, New Zealand, the Pacific islands, and the tip of South America the chance to detect events on land down to this size at (at least) four stations is higher than 80 per cent.

b. Extension of Amplitude-Attenuation Curves beyond 100 deg Distance

The most prominent result of the last section is the clear difference in detection capability between northern and southern hemisphere regardless what type of attenuation function was applied in the teleseismic window. To reduce the detection threshold in the southern hemisphere a substantial increase of the number of stations in that region has often been recommended. Although this is a solution in principle, there are several practical problems with its realization. The major part of the southern hemisphere is covered by deep ocean areas where installation and maintenance of seismographs is still difficult and expensive. Islands are known for a high microseismic noise level and poor detection capability.

An attractive alternative for improving the detection capability in the southern hemisphere is provided by signals which have travelled through the earth's core and are routinely detected at stations beyond 100 deg distance. In a specific window, i.e., $142\ deg < \Delta < 152\ deg$ these refracted core phases offer even better detection possibilities than earlier described direct p-waves. Numerous studies have shown that observation of high amplitudes for various pkp-branches can be a powerful tool in lowering detection thresholds. (Blandford and Sweetser, 1973), (Quamar, 1973.) This can easily be demonstrated with a seismogram of a French clear underground explosion exploded at Mururoa atoll (21 S,140 W) and recorded with the Graefenberg array in Germany ($\Delta = 143.7 deg$). Figure 9 shows a recording at all 13 vertical elements of the array (for a more detailed description see Harjes and Seidl, 1978) and the beam-trace on top from which a displacement amplitude of 4 nm at a period of 0.8 sec was measured.

In comparison Figure 10 shows recordings of the same event by the RSTN-stations in North America. These stations (Engdahl et al., 1982) are new borehole installations and include seismometers (Geotech S-750) with high sensitivity in the short-period band. Traces are aligned to the theoretical arrival time of the p-wave which is marked by the cursor line. The stations have a distance of 73 deg to 88 deg from the event. Neither the original (upper part) nor the narrow-band filtered (lower part) traces meet the

detection requirements set in our calculations. Correspondingly, this event was not reported by international data centers which restrict their event-defining association process to p-arrivals within 100 deg distance.

Figure 11 shows the summary of station reportings for this event available from GTS/WMO-channels at the CSS. The association program implemented at the CSS found the questionable event by using pkp-observations from three stations in Europe (including GRF). With the detection criterion we applied in the preceding paragraph (at least 4 p-detections) this event would have been missed.

Consequently, we amended amplitude-distance curves beyond 100 deg as shown in Figure 12. There are two curves from different sources (Blandford and Sweetser, 1973), (Ringdal, 1984) which show a great similarity although Blandford and Sweetser's curve is based on a much more general data base (ISC) than Ringdal's data which are derived only from NORSAR observations. Detection threshold estimates for the 50-station network calculated with these attenuation curves differ less than 0.1 magnitude unit. Israelsson, (1984) recommended the requirement of at least one p detection additional to pkp-arrivals to define an event to avoid large location errors because the stations observing pkp might be clustered in a narrow geographical area. Figure 13 gives the network detection capability for detecting at least 4 p- or pkp-arrivals, one of which has to be a direct p-wave, i.e., observed at a station within less than 100 deg distance of the event. This result can directly compared with Figure 3 because the attenuation functions are identical up to 100 deg distance.

The inclusion of pkp-phases yields a large decrease of the detection threshold for the southern hemisphere (0.3 to 0.5 magnitude units) and divides the difference in detection capability between northern and southern hemisphere by half compared to the only use of p-arrivals within 100 deg distance.

c. Variation of Amplitude-Attenuation Curves at Regional Distances

In discussing the influence of varying teleseismic attenuation functions on the network detection capability we always used the same curve for regional distances (Δ<25 *deg*). Although the teleseismic part (including pkp) will be most important for a global network regional differences will have some effect in areas (Europe and Scandinavia) where the 50-station network is highly represented. These areas give us the opportunity to study the effect of different regional attenuation functions which, in a gross sense, represent "stable" (i.e., high Q) and "tectonic" (i.e., low Q) provinces.

The distinction was initially introduced for the North American continent taking into account the different crustal structure in western and eastern U.S. (Evernden, 1967). In this section we discuss only the influence of variations of p_n-wave which is seen as the first arrival on regional

seismograms recorded at distances greater than 1 deg. To emphasize the difference rather extreme representatives of published attenuation curves have been used, namely Evernden's "8.5" curve (Evernden, 1967) derived from data in the eastern U.S. (b=-0.83, c=-2 in Equation (3)) compared to a p_n attenuation curve d[illegible]d from data in southwestern U.S. (Der et al., 1982) which yield b=0.1[illegible] and c=-3.803. Thus, th[illegible] main difference between these two types of regional attenuation curves is that the "stable" p_n drops off as the square of the distance while the "tectonic" curve decreases more rapidly, almost with the fourth power of the distance.

Another peculiarity at regional distances is the relative maximum in the amplitude-distance curve as a result of the 20 deg discontinuity which is observed worldwide with differing prominence (Gutenberg and Richter, 1956), (Veith and Clawson, 1972). To emphasize also the effect of the 20 deg discontinuity the Veith-Clawson curve has been appended to Evernden's curve in the distance range 17 $deg<\Delta<25$ deg. On the opposite side the "tectonic" attenuation curve has been smoothly connected to teleseismic distances without consideration of a 20 deg discontinuity.

Our final regional extensions of attenuation functions are plotted in Figure 14. It is again noted that these curves are artificial compositions to show the most pronounced effect on network detection capability. The result can be seen in Figure 15 and Figure 16 which are to be compared to Figure 13. Using specified regional attenuation curves generally increases the influence of station distribution. Global differences of detection thresholds are pronounced in Figure 15 which shows the influence of a "stable" (Evernden "8.5"+ 20 deg disc.) regional attenuation curve. At close-to-station distances detection thresholds are decreased by up to 0.2 magnitude units as compared to Figure 13. On the contrary detection thresholds are increased for most parts of Eurasia and America by up to 0.2 magnitude units for a "tectonic" attenuation curve (Figure 16). Worldwide, this attenuation curve smoothes the difference in detection capability between northern and southern hemisphere, certainly a result of our station distribution.

In summary regional variation of amplitude attenuation curves can change the detection threshold of a global 50-station network by as much as ± 0.2 magnitude units.

IV. Regional Detection Probabilities of a Global Network

Although this paper mainly deals with teleseismic detection capabilities it is interesting to investigate to what extent the magnitude threshold of a global network will be influenced by including other than p_n phases. It should be mentioned at the beginning that this section is intended as an amendment to teleseismic capabilities. To study the full potential of regional waves for detection purposes a regional station network has to be

introduced. This is beyond the scope of this report and for details on this matter we refer to excellent recent review articles (Pomeroy et al., 1982), (Blandford, 1981).

It is well known that the largest amplitudes on a short-period regional seismogram occur within the lg-wavetrain which may be interpreted as a superposition of a large number of higher mode Love and Rayleigh waves - lg-amplitudes can be ten times larger than the maximum amplitude of the first arrival (p-wave) at the same distance and in the same period band around one sec. The actual amplitude can drastically vary due to local geology. An extensive literature exists on amplitude-distance attenuation curves for lg for various regions of the world (for reference see the above mentioned review articles).

Again, we extract two extreme representatives of published curves to examine the effect on the detection capability. As representing "stable" regions with low attenuation we choose an attenuation curve published by Nuttli, (1973). Nuttli derived an amplitude decay with distance proportional to $\Delta^{-5/3}(0.5deg<\Delta<40deg)$ corresponding to the shape of well-known "Prague"-formula (Vanek et al., 1962) adopted by IASPEI to be used for teleseismic Rayleigh wave observations. However, Nuttli derived his curve from observations of one1 sec lg-waves in the eastern U.S., whereas the "Prague"-formula is valid for Raleigh waves around 20 sec.

For crustal structures in "tectonic" provinces like the western U.S. an amplitude-distance decay for lg proportional to Δ^{-3} was observed (Der et al., 1982). The selected attenuation curves are plotted in Figure 17. In estimating detection capabilities by use of lg-waves it has to be mentioned that its amplitude is not only regionally varying but that it also can be totally squelched. Representing a wave guide phenomenon lg-propagation is seriously effected by variations in crustal thickness (mountains,ocean-continent and/or tectonic boundaries). To take these inefficient wave paths into account a much finer than the 15 deg x 15 deg grid used in our calculations has to be applied.

We want to examine whether inclusion of lg-waves has an effect on a global network at all. If there appear regional improvements of the detection capability these have to be verified by considering the corresponding regional crustal structure. Because we want to insist on teleseismic detections we use lg-detections only if at least one station of the network observed a teleseismic p-wave ($\Delta>25$ deg). So we required at least two lg-detections and 1 teleseismic p-detection or four p-detections. As lg is observed on all three components of ground motion an azimuth estimate can be calculated and two stations are sufficient to roughly associate the event origin. An event is declared if at least one p-observation at teleseismic distances confirms this association.

Figure 18 and Figure 19 show the detection capability using this criterion for Nuttli's and Der et al.'s attenuation function respectively, in comparison to Figure 15 and Figure 16 which show the corresponding p-wave detection results thresholds are lowered by 0.1 to 0.3 magnitude units. Again, it should be emphasized that these improvements are irrelevant if they occur in oceanic areas because lg-waves disappear after crossing approximately 100 km of oceanic structure. Restricting the evaluation to continental areas only it can be seen from Figure 18 and Figure 19 that the detection threshold is mostly influenced in the southern hemisphere where occasionally two stations are located

at regional distances. In Europe and Scandinavia we reach already a high capability for four p-detections which is not significantly improved by the additional (two lg and one teleseismic)-detection probability. Finally, it might be mentioned that the detection difference caused by the difference of the two attenuation curves (Figure 17) is only marginal.

V. Station Data

After discussing the influence of amplitude-distance curves on network detection capability the remaining factor which determines detection thresholds is the noise statistics of stations. Published magnification curves or spectral estimates from short time windows formed the basis to estimate these values. More reliable data can be obtained by actually measuring the performance of each station over an extended period of time. Unfortunately noise measurements are not reported regularly by stations, so an indirect method was applied to estimate those from station detection thresholds. The data base of the International Seismological Centre (ISC) for 1980 was used as a reference system and station detection values computed by Ringdal, (1984) were taken to derive station noise values. The following procedure was used:

- given : station detection threshold log A/T
- calculate : amplitude of detection threshold A at T = one sec
- assume : signal-to-noise ratio r for detection
- deduce : station noise amplitude

Before discussing the result of this procedure it has to be verified that the selected stations reported to the ISC in 1980. In column 6 of Table 1 the number of teleseismic detections published by ISC is listed for all stations belonging to the 50-station network. Of course no noise estimate can be deduced for stations which do not appear in this list. Fortunately, for some stations we could find a nearby substitute. They can be recognized from Table 1 having additional station names in brackets which were the original ones selected in our 50-station network. Finally, we were able to calculate "operational" noise statistics (MLE-SP noise in Table 1) for 40 stations which can be seen to differ substantially from earlier estimated figures (column 4 and 5 of Table 1). The difference can easily be demonstrated in Figure 20 which shows a histogram of noise data we used in network detection studies as thick lines compared to our new values (dotted lines.) derived from Ringdal's maximum-likelihood estimates (MLE) of station detection thresholds. The "operational" noise values represent much closer a normal distribution peaked around 0.8-0.9 (corresponding to 6 nm - 8 nm) than the original data which showed 12 stations with a mean noise value of 2 nm. It might be mentioned that the shift of very sensitive stations (like LAO and NAO) is biased by taking the ISC-bulletin as reference because part of their detections do not meet the event defining criteria of the center. But this restriction of our procedure has little influence on the following discussion as the network capability is largely determined by the general increase of noise values.

To elaborate further on this difference of noise estimates we examined data from our German station at Graefenberg (GRF). We could use an adequate data set while

GRF participated in a Common Data Base Experiment (CDBE) which was conducted by Sweden under the auspices of the Geneva group of seismologists during the time period Oct 1 - Oct 15 1980 (Barkeby et al., 1981). Figure 21 shows a power spectral density (PSD) plot of noise measured at GRF during the time period of that experiment. This spectrum represents an average over 20 noise samples taken in time intervals of four min between 00:00 h and 01:30 h on Oct 10. Each noise sample was computed from a time series of 2048 values (Δt=0.05sec) multiplied by a cosine-window. We read $0.4nm^2/Hz$ at 1 Hz from this PSD-plot. Assuming normal distributed noise we calculate an average zero-to-peak noise amplitude using following formula (Taylor, 1981).

$$average0-p-amplitude \approx [2BW(Hz)\cdot\Phi(f)(A^2/Hz)]$$

where BW is the bandwidth of the recording system and $\Phi(f)$ is the power spectral density. With BW = 5 Hz for GRF-seismograph and Φ=$0.4nm^2/Hz$ we get

$$average0-p-amplitude \approx 2nm$$

a value which in fact was supplied for network capability calculations in 1978 (CCD/558) as can be seen from Table 1 (column 4).

During the Common Data Base Experiment stations were asked to report noise measurements in addition to standard parameters and were instructed to read the maximum noise value within 30 sec preceding the p-wave (in the frequency band of the signal).

Figure 22 shows a histogram of these noise amplitudes (Hanka and Henger, 1980) for station GRF. Although this data set is rather limited (70 values), and not well represented by a normal distribution, a calculation of mean and standard deviation shows good agreement with Ringdal's figure (Table 1). Besides it can be seen from Figure 22 that there is a smaller peak of measurements at about 0.3 (the value derived from PSD-data). The majority of data, however, is shifted about 0.5 to higher noise values.

If we assume that the procedure demonstrated for GRF is generally applicable then the conclusion can be drawn that average 0-p-amplitude noise values (from PSD-estimates) are not appropriate as input data in the detection calculations but rather that the actually measured maximum 0-p-values, taken over many samples, are required. Of course, this conclusion is closely related to the specified signal-to-noise ratio r = 1.5 at which stations are assumed to detect an event. In the algorithm (Equation 1) one could always compensate for systematically low noise estimates by increasing s/n-ratio to r = 5 (for example). Commonly a value of r = 1.5 is more acceptable if correct noise data can be found.

Thirty-nine stations (marked by an asterisk in Table 1) were used to compare our results from the "model network" with real station data. The geographical distribution of these 39 stations can be seen in Figure 23. To some extent this reduced network

represents a more even global coverage than the 50-station network. At first we examined the effect of the reduction in station number. Figure 24 shows the detection capability of this reduced network which is directly comparable to Figure 3 because the same attenuation curve and same station data were used. Although we have earlier reported from previous studies that a smaller network of high-quality stations is preferable to the full use of all worldwide existing stations the small effect of reducing our 50-station network by more than 20 per cent is still surprising. The difference of detection threshold is at most 0.1 magnitude unit and therefore negligible within the numerical precision of our results.

A significant change is, however, accomplished if the new station data (noise statistics) are introduced (Figure 25). Magnitude thresholds are increased by about half a magnitude unit. Ringdal (personal communication, 1984) used his station detection thresholds and recurrence estimates from observed earthquakes in 1980 to obtain detectability thresholds for regions with sufficient number of observations (Kelly and Lacoss, 1969). His results for the same network are shown in brackets on Figure 25 and a very good agreement to our data can be found. The remaining differences are well explained by the different methods and should not been further interpreted.

VI. Conclusions

Estimation techniques to examine seismic network detection capabilities including multiwave detection criteria are well established. For a representative global 50-station network - composed by an international group of seismologists (CCD/558, 1978) and further studied in this report - magnitude thresholds requiring a 90 per cent probability of at least four detecting stations range from:

$3.4 \leqslant m_b \leqslant 3.6$ for Scandinavia and Europe
$3.7 \leqslant m_b \leqslant 4.0$ for North America, Asia, and Arctica
$3.8 \leqslant m_b \leqslant 4.3$ for South America, Africa, and Antarctica
$4.0 \leqslant m_b \leqslant 4.6$ for Australia, New Zealand, and Pacific.

Current teleseismic detection thresholds are at least half a magnitude unit higher. The discrepancy between model results and actual reportings can be explained by adjusting station data. These data have more influence on global detection thresholds than variation of amplitude-distance curves within reasonable bounds. After estimation of noise statistics from long observation intervals predicted magnitude detection thresholds and empirical values are in good agreement.

Considerable improvements of existing seismological instrumentation and practice is needed to achieve those values predicted from the model network:

- To lower the background noise of stations we recommend installation of seismometers in boreholes or use of miniarrays which offer the additional benefit of phase identification.

- Station noise should be permanently monitored by reporting noise values in connection with conventional station readings.

- Automated detector algorithms should be implemented at all stations.

- Data centres should use all relevant information for defining events, i.e., use more than p-phases (especially pkp) in association process.

- Amplitude attenuation tables for all distances should be standardized to specific frequency bands and applied to amplitude measurements from identical instrument responses.

With these modifications a global 50-station network is assumed to come up to teleseismic detection thresholds as predicted from our calculations.

VII. Acknowledgments

This work was carried out during a visit at the Center for Seismic Studies in Arlington, Virginia. The author is especially indebted to R. Alewine and A. Kerr from the U.S. Advanced Defense Research Projects Agency for their kind invitation. The support of C. F. Romney and the entire staff at the CSS is gratefully acknowledged. Many of the ideas in this paper resulted directly or indirectly from discussions with F. Ringdal to whom the author is deeply indebted. He further wishes to thank R. Suey, Pacific-Sierra Research, for his support in making SNAP/D run at the Center.

VIII. REFERENCES

Barkeby, G., Bergkvist, N. O., Dahlman, O., Johansson, P., Ohlsson, H., and Roy, F., 1981. "Common Data Base Experiment," *Progress Report on Data Analysis, FOA-Report*, C-20431-T1, Stockholm, Sweden.

Basham, P. W. and Whitham, K., 1970. "Seismological Detection and Identification of Underground Nuclear Explosions," *Report, EPB, Department of Energy, Mines and Resources*, Ottawa, Canada.

Blandford, R. R. and Sweetser, E. I., 1973. "Seismic Distance-Amplitude Relations for Short Period P, Pdiff, PP and Compressional Core Phases for Delta > 90 Deg.," *Report, Teledyne-Geotech*, SDAC-TR-73-9, Alexandria, VA.

Blandford, R. R., 1981. "Seismic Discrimination Problems at Regional Distances," *NATO, Advanced Study Institutes*, Series C, 74, D. Reidel Publ. Comp., Dordrecht, Holland.

CCD/558, 1978. "Report to the Conference of the Committee on Disarmament of the Ad Hoc Group of Scientific Experts to Consider International Co-Operative Measures to Detect and to Identify Seismic Events," Geneva, Switzerland.

Ciervo, A. P., Sanemitsu, S. K., Snead, D. E., and Suey, R. W., 1983. "Seismic Network Assessment Program for Detection," *Report 1027A, Pacific-Sierra Research*, Los Angeles, CA.

Davies, D. (Rapporteur), 1969. "Seismic Methods for Monitoring Underground Explosions," *SIPRI*, Stockholm, Sweden.

Der, Z. A., O'Donnell, A., McElfresh, T. W., Julita, R., Burnetti, J. A., Marshall, M., Silk, M., and Gordon, E., 1982. "A Study of Seismic Wave Propagation at Regional Distances in Five Areas of the World," *Report, Teledyne-Geotech*, VSC-TR-82-14, Alexandria, VA.

Elvers, E., 1978. "The Capability of a Network of Seismological Stations to Detect Events and to Obtain Identification Parameters," *FOA-Report*, C-20231-T1, Stockholm, Sweden.

Engdahl, E. R., Peterson, J., and Orsini, N. A., 1982. "Global Digital Networks-Current Status and Future Directions," *BSSA*, 72B, S243-S260.

Evernden, J. F., 1967. "Magnitude Determination at Regional and Near-Regional Distances," *BSSA*, 57, 591-639.

Evernden, J. F. and Clark, D. M., 1970. "Study of Teleseismic P. II.-Amplitude Data," *Phys. Earth Planet. Int.*, 4, 24-31.

Gutenberg, B. and Richter, C. F., 1956. "Magnitude and Energy of Earthquakes," *Ann. Geofis.*, 9, 1-15.

Hanka, W. and Henger, M., 1980. "Experiment zur routine maessigen Bestimmung von seismischen Level-1 Parametern," *Report-86997, BGR*, Hannover, F. R. Germany.

Harjes, H.-P. and Seidl, D., 1978. "Digital Recording and Analysis of Broad-Band Seismic Data at the Graefenberg (GRF)-Array," *J. Geophys.*, 44, 511-521.

Israelsson, H., 1984. "Experiments with a Computer Program for Automatic Association of Seismic Events," Unpublished Manuscript.

Kelly, E. J. and Lacoss, R. T., 1969. "Estimation of Seismicity and Network Detection Capability," *Technical Note 1969-41*, Lincoln Lab, MIT, Mass.

Lacoss, R. T., Needham, R. E., and Julian, B. R., 1974. "International Seismic Month Event List," *Technical Note 1974-14*, Lincoln Lab., MIT, Mass.

Marshall, P. D. and Basham, P. W., 1972. "Discrimination between Earthquake and Underground Explosions Employing an Improved Ms Scale," *Geophys. J.*, 28, 431-458.

NORSAR

Nuttli, O. W., 1973. "Seismic Wave Attenuation and Magnitude Relations for Eastern North America," *J. Geophys. Res.*, 78, 876-885.

Pomeroy, P. W., Best, W. J., and McEvilly, T. V., 1982. "Test Ban Treaty Verification with Regional Data - A Review," *BSSA*, 72B, S89-S130.

Quamar, A., 1973. "Revised Velocities in the Earth's Core," *BSSA*, 63, 1073-1105.

Ringdal, F., Husebye, E. S., and Fyen, J., 1977. "Earthquake Detectability Estimates for 478 Globally Distributed Seismograph Stations," *Phys. Earth Planet. Int.*, 15, 24-32.

Ringdal, F., 1984. "Study of Magnitudes, Seismicity, and Earthquake Detectability Using a Global Network," Unpublished Manuscript.

Taylor, S. R., 1981. "Properties of Ambient Seismic Noise and Summary of Noise Spectrum in the Vicinity of RSTN Sites," *Report UCID*, Lawrence Livermore Lab., Livermore, CA.

US/GSE/7, 1980, "Investigation of the Properties of CD-Network III Using Synthetic Data," *Report of the United States Delegation*, Geneva, Switzerland.

Vanek, J., Zatopek, A., Karnik, V., Kondorskaya, N. V., Riznichenko, Y. V., Savarenski, E. F., Solov'ev, E. L., and Shebalin, N. V., 1962. "Standardization of Magnitude Scales," *Bull. (Izvest.) Acad. Sci. USSR*, Geophys. Ser., 2, 108.

Veith, K. F. and Clawson, G. E., 1972. "Magnitude from Short-Period P-Wave Data," *BSSA*, 62, 435-452.

Wirth, M. H., 1977. "Estimation of Network Detection and Location Capability," *Report, Tele lyne-Geotech*, Alexandria, VA.

STATION CODE	LAT +=N	LONG +=E	SP-NOISE MEAN	SP-NOISE STD	TELES. DETECTIONS	MLE-SP-NOISE MEAN	MLE-SP-NOISE STD	ISC NETWORK
AFI	-13.91	-171.78	1.48	0.50	217			
ALE	82.48	-62.40	0.70	0.40	546	0.70	0.21	•
ALQ	34.95	-106.46	0.30	0.20	1393	0.78	0.24	•
ANP(TATO)	24.97	121.48	0.60	0.35	153	1.11	0.20	•
ANTO	39.92	32.82	0.30	0.20	182	0.95	0.20	•
ARE	-16.46	-71.49	0.85	0.45	222	1.0	0.15	•
ASP	-23.68	133.90	0.48	0.30	1801	1.08	0.31	•
BAO(BDF)	-15.66	-47.90	0.30	0.20	301	0.78	0.16	•
BNG	4.37	18.57	0.00	0.15	729	0.60	0.18	•
BOG(BOCO)	4.57	-74.04	0.30	0.20	188	0.70	0.20	•
BOD	57.85	114.18	0.70	0.40	971	0.85	0.12	•
BUL	-20.14	28.61	0.60	0.35	666	0.70	0.10	•
CHG(CMT)	18.90	98.98	0.30	0.20	2072	0.90	0.23	•
COL	64.90	-147.78	0.70	0.40	2335	0.60	0.12	•
COM	16.15	-92.07	1.00	0.50				
DAG	76.77	-18.77	1.08	0.50	1041	0.85	0.15	•
EKA	65.33	-3.16	0.90	0.45	559	0.85	0.26	•
ELT	53.25	86.27	0.70	0.40	825	0.85	0.20	•
GBA	13.60	77.40	1.18	0.50	1782	0.90	0.25	•
GRF	49.69	11.21	0.30	0.20	536	0.78	0.26	
HFS	60.13	13.70	0.00	0.15	1803	0.48	0.22	•
IFR	33.31	-5.07	0.70	0.40				
KJF(JYS)	62.17	24.67	0.30	0.20	1696	0.60	0.10	•
KHC	49.13	13.58	0.48	0.30	979	0.70	0.20	•
KIC	6.36	-4.74	0.48	0.30	782	0.70	0.20	•
KSR	38.00	128.00	0.48	0.30				
LAO	46.6?	-106.22	-0.40	0.15	1163	0.3	0.25	•
MAIO	36.31	59.59	0.30	0.20	1046	0.78	0.16	•
MAT	36.54	138.21	1.00	0.50	911	0.95	0.19	•
MAW	-67.60	62.88	1.00	0.50	330	0.95	0.27	•
MBC	76.24	-119.36	0.78	0.45	1550	0.48	0.26	•
NAI(NIK)	-1.27	36.80	0.30	0.20	127	1.08	0.20	•
NAO	61.04	11.22	-0.10	0.15	1247	0.30	0.24	•
NIE	49.41	20.31	0.70	0.40	138			
OBN	55.17	36.60	0.78	0.45	728	0.78	0.17	•
OTT(GAC)	45.40	-75.67	0.30	0.20	108	1.04	0.50	•
PNS	-16.27	-68.47	0.48	0.30				
QUE	30.18	66.95	0.70	0.40				
SBA	-77.85	166.76	1.48	0.50	863	1.0	0.20	•
SHL	25.57	91.88	0.30	0.20	947	1.08	0.13	•
SNA	-70.32	-2.33	1.18	0.50	125	1.18	0.20	•
SPA	-89.90	0.10	0.90	0.40	1188	0.85	0.31	•
SVE	56.80	60.63	0.70	0.40	869	0.85	0.19	•
TAM	22.79	5.52	0.60	0.35				
TLL	-30.10	-70.48	1.00	0.50				
WEL	-41.29	174.78	1.48	0.50	150	1.48	0.20	•
WES	42.38	-71.32	1.00	0.50				
WRA	-19.95	134.35	0.30	0.20	3169	0.70	0.26	•
YAK	62.02	129.72	0.70	0.40	1015	1.04	0.20	•
YKA	62.49	-114.60	0.48	0.30	1727	0.70	0.18	•

Table1. Stations used in network-detection capability computations with noise statistics(mean and standard deviation of logarithm). Different estimates are explained in the text.

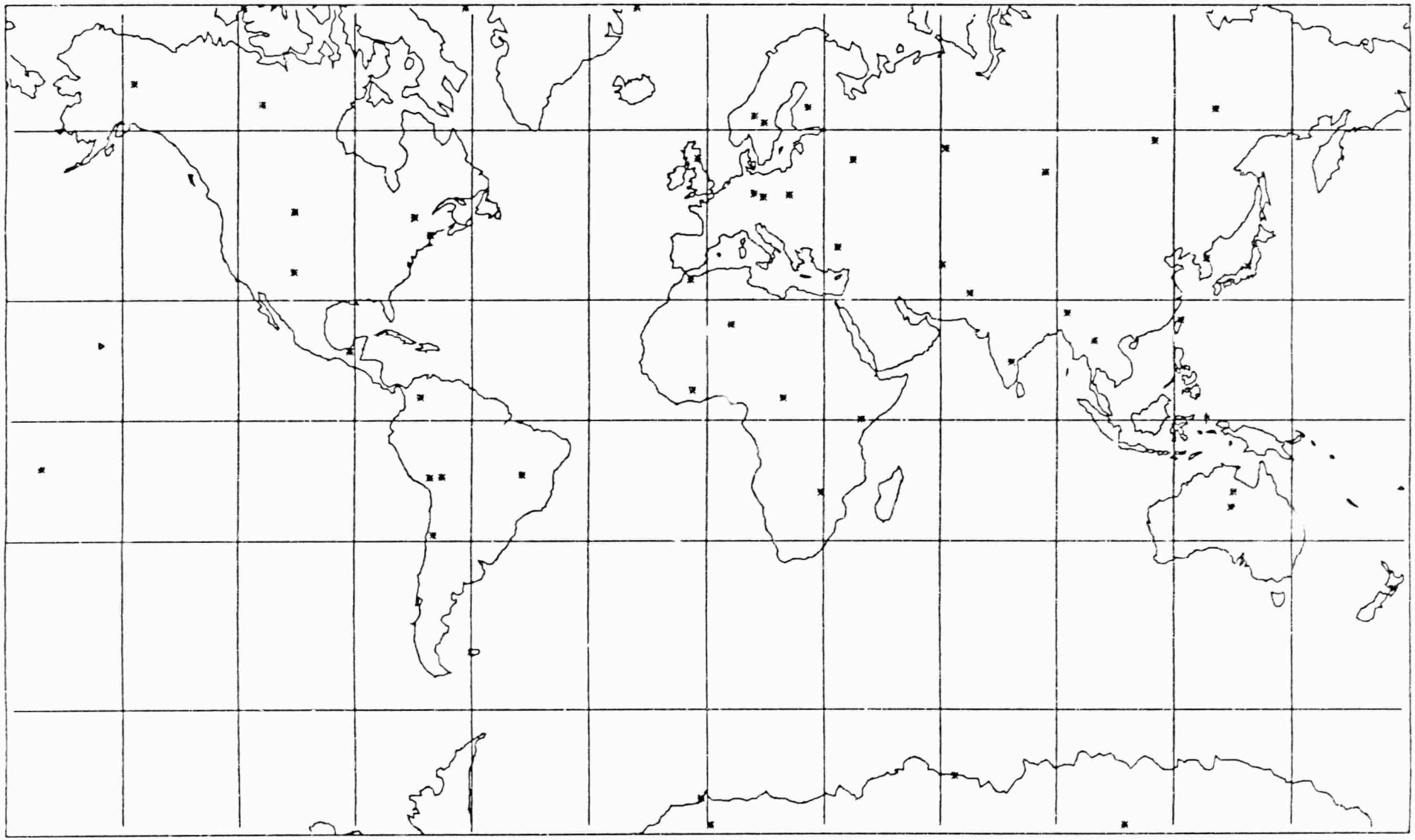

Fig. 1: Global Seismic Network (50 stations from CCD/558 (1978))

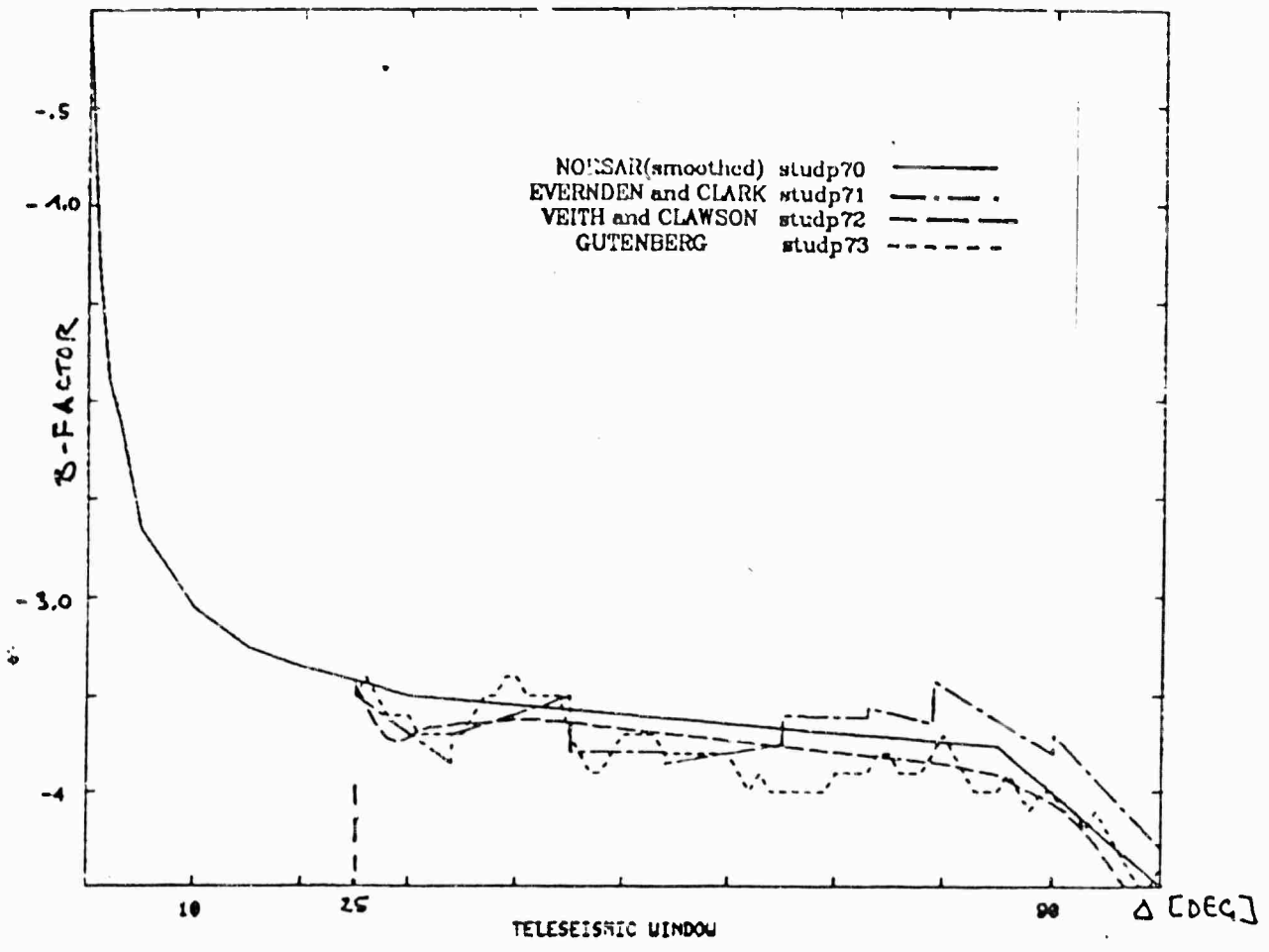
NORSAR(smoothed) studp70
EVERNDEN and CLARK studp71
VEITH and CLAWSON studp72
GUTENBERG studp73
-.5
-1.0
-3.0
-4
B-FACTOR
10
25
90
Δ [DEG]
TELESEISMIC WINDOW

Fig. 2

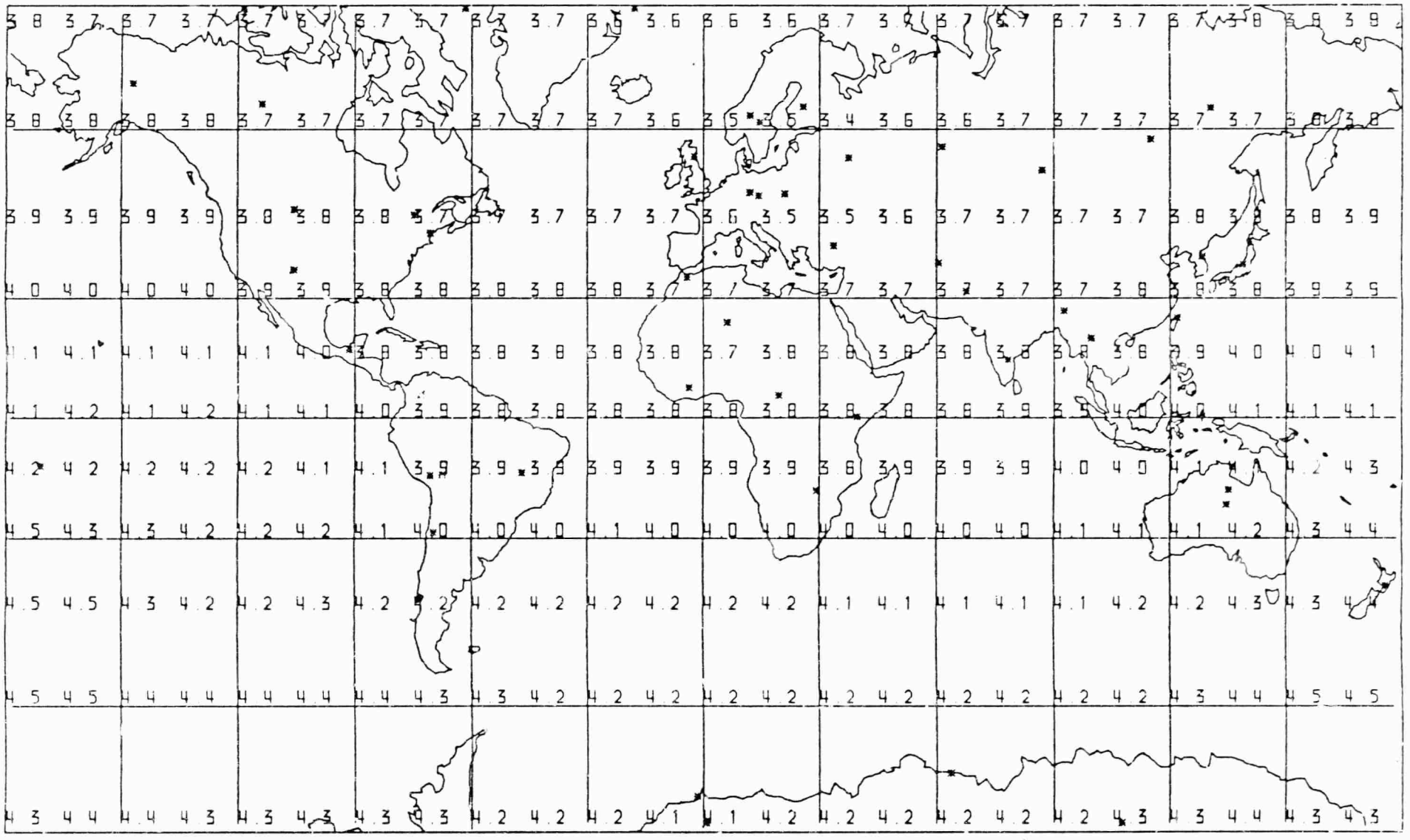

Fig. 3: 50-station p/4-thresh prob =0.9 studp70 atten curve

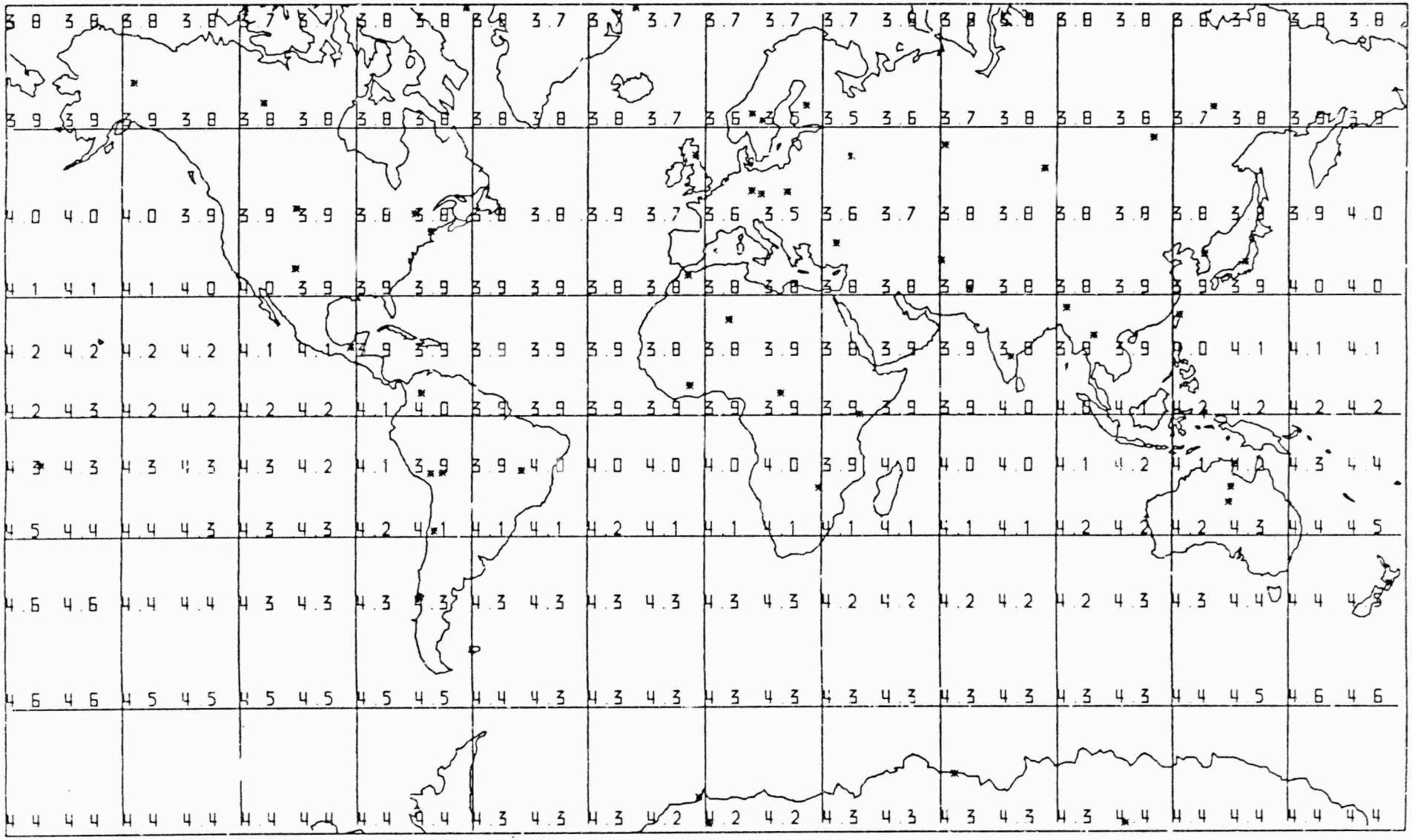

Fig. 4. 50-station p/4-thresh prob =0.9 studp72 atten curve

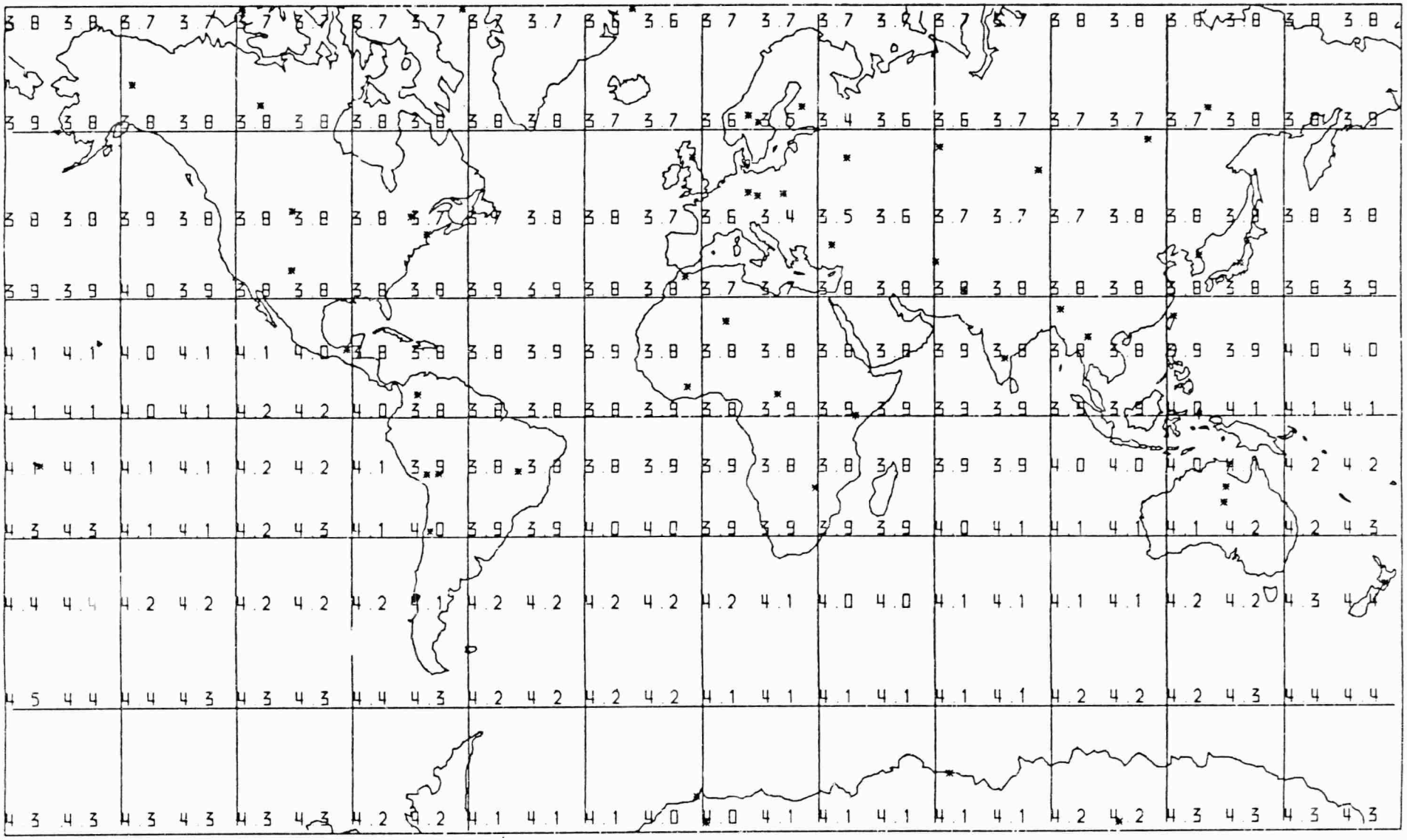

Fig 5: 50-station p/4-thresh prob =0.9 studp71 atten curve

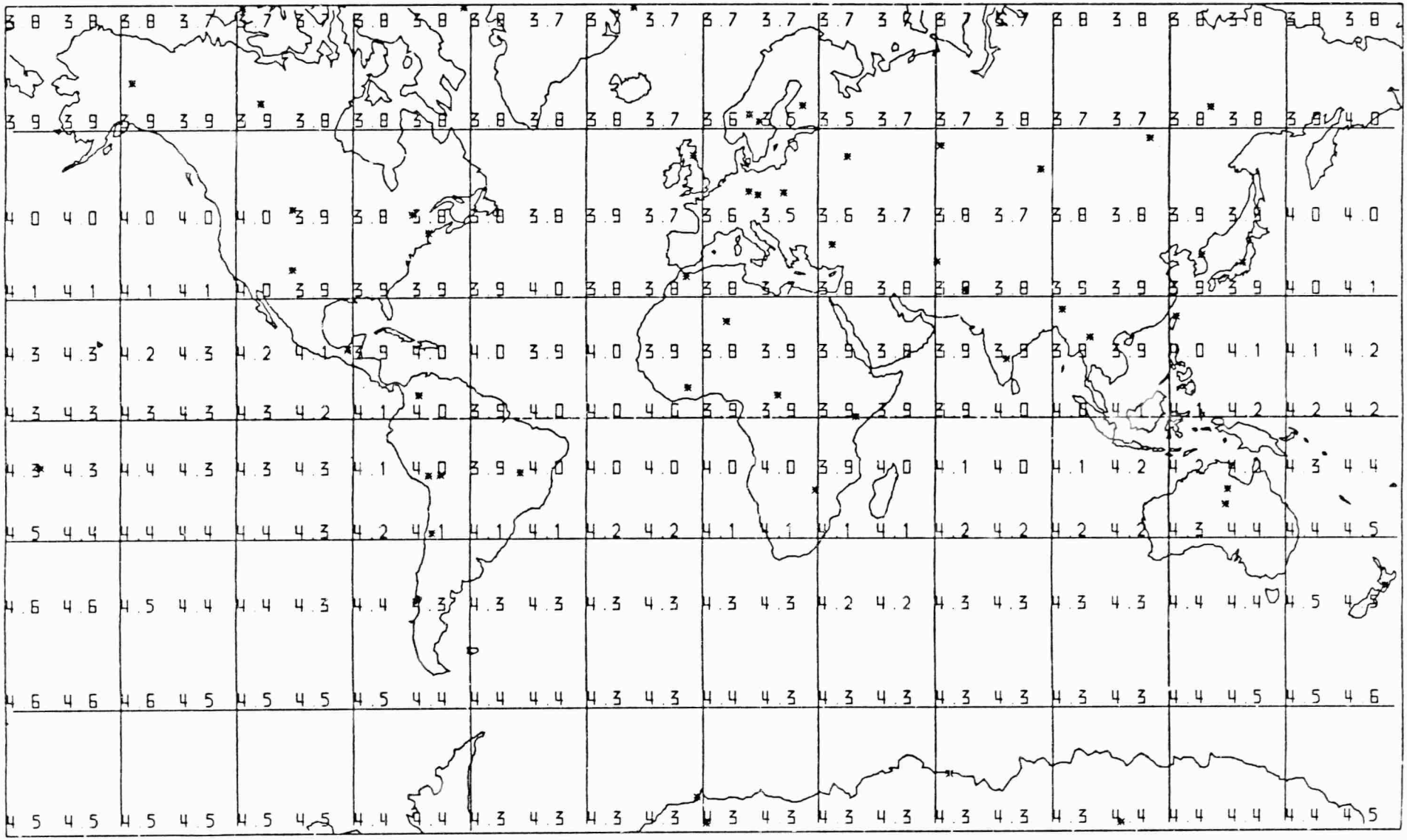

Fig. 6: 50-station p/4-thresh prob. =0.9 studp73 atten curve

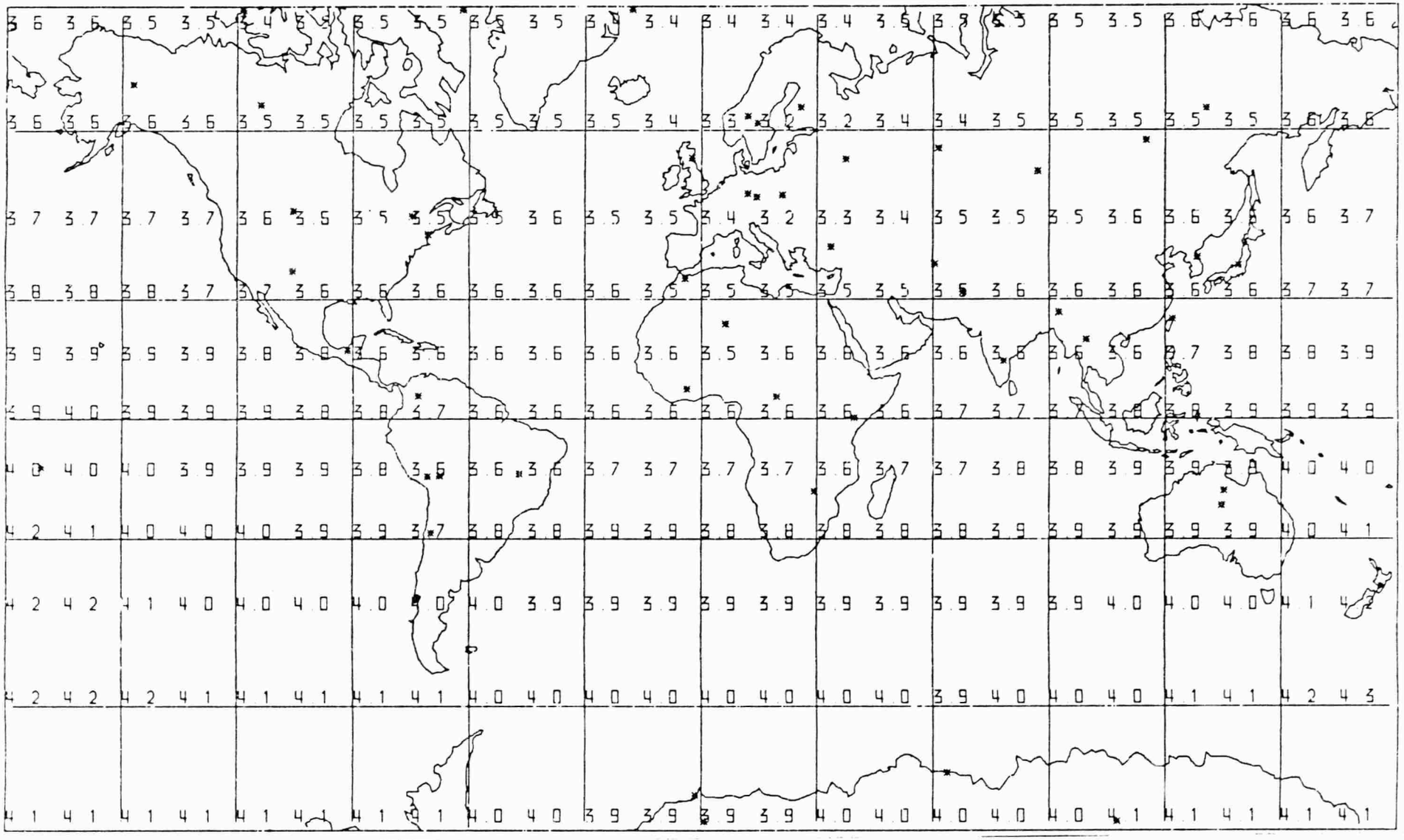

Fig.7 : 50-station p/4-thresh prob =0.3 studp70 atten curve

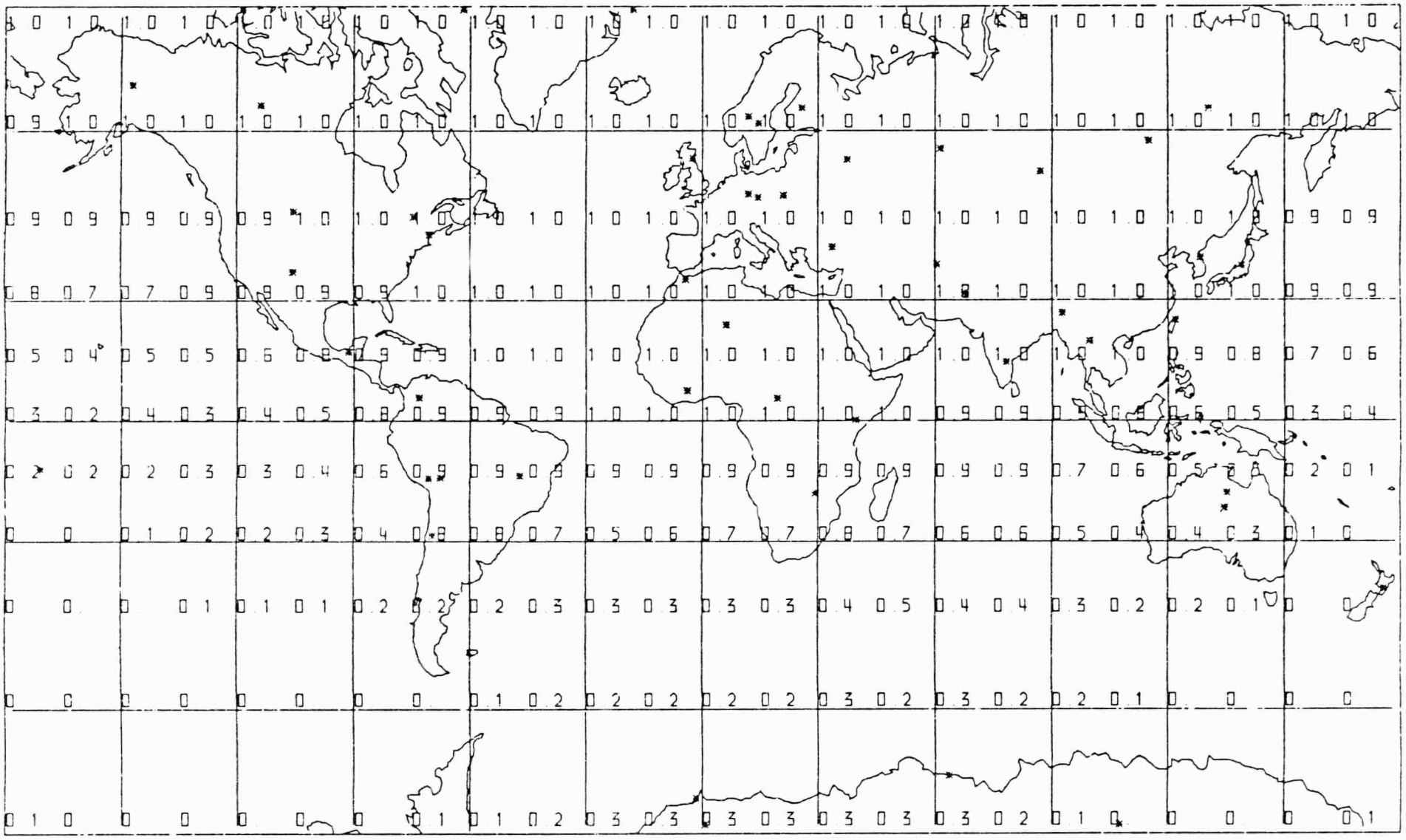

Fig. 8 50-station p/4-thresh magn =4.0 studp70 atten curve

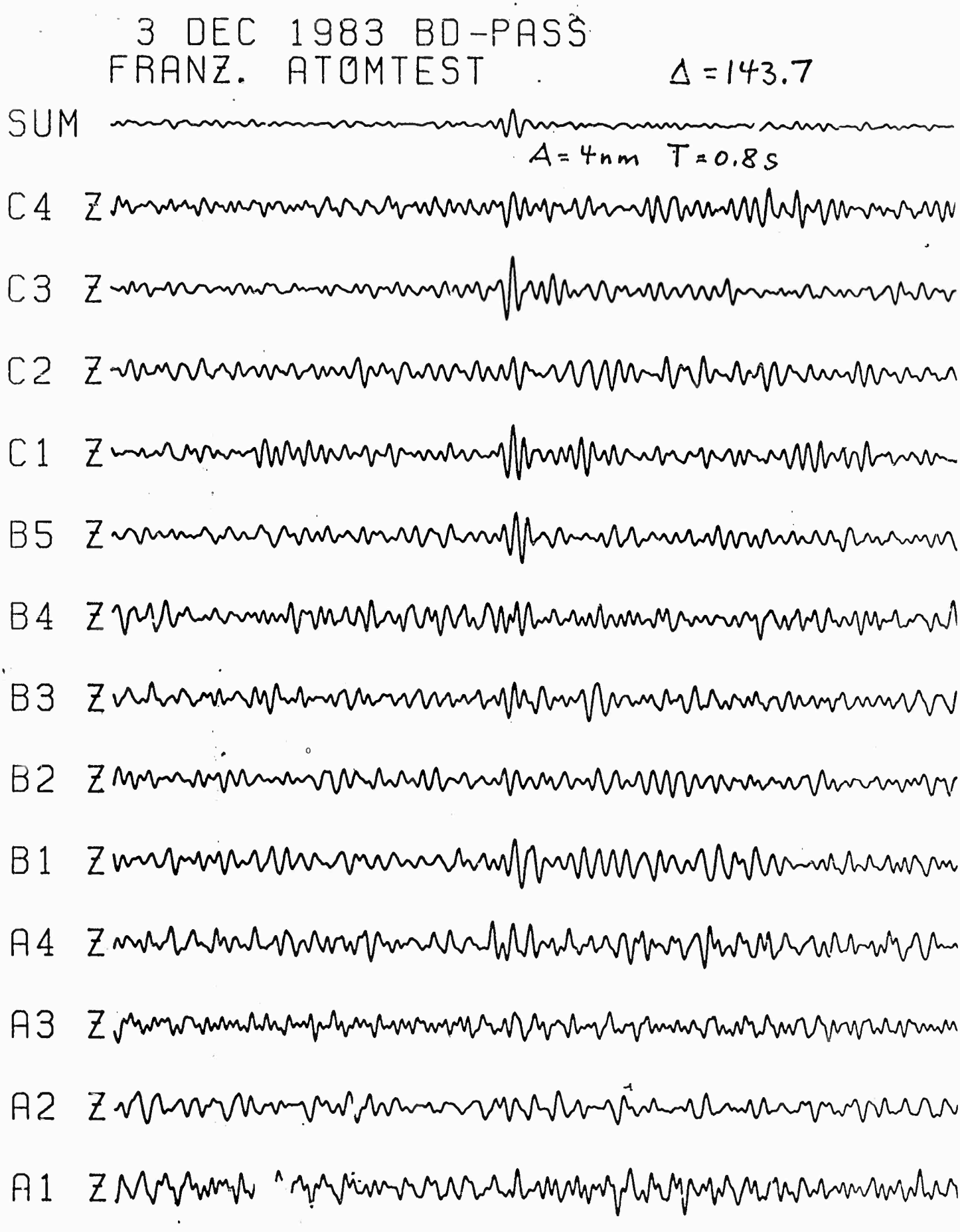

Fig. 9: French nuclear test recorded with GRF-array.

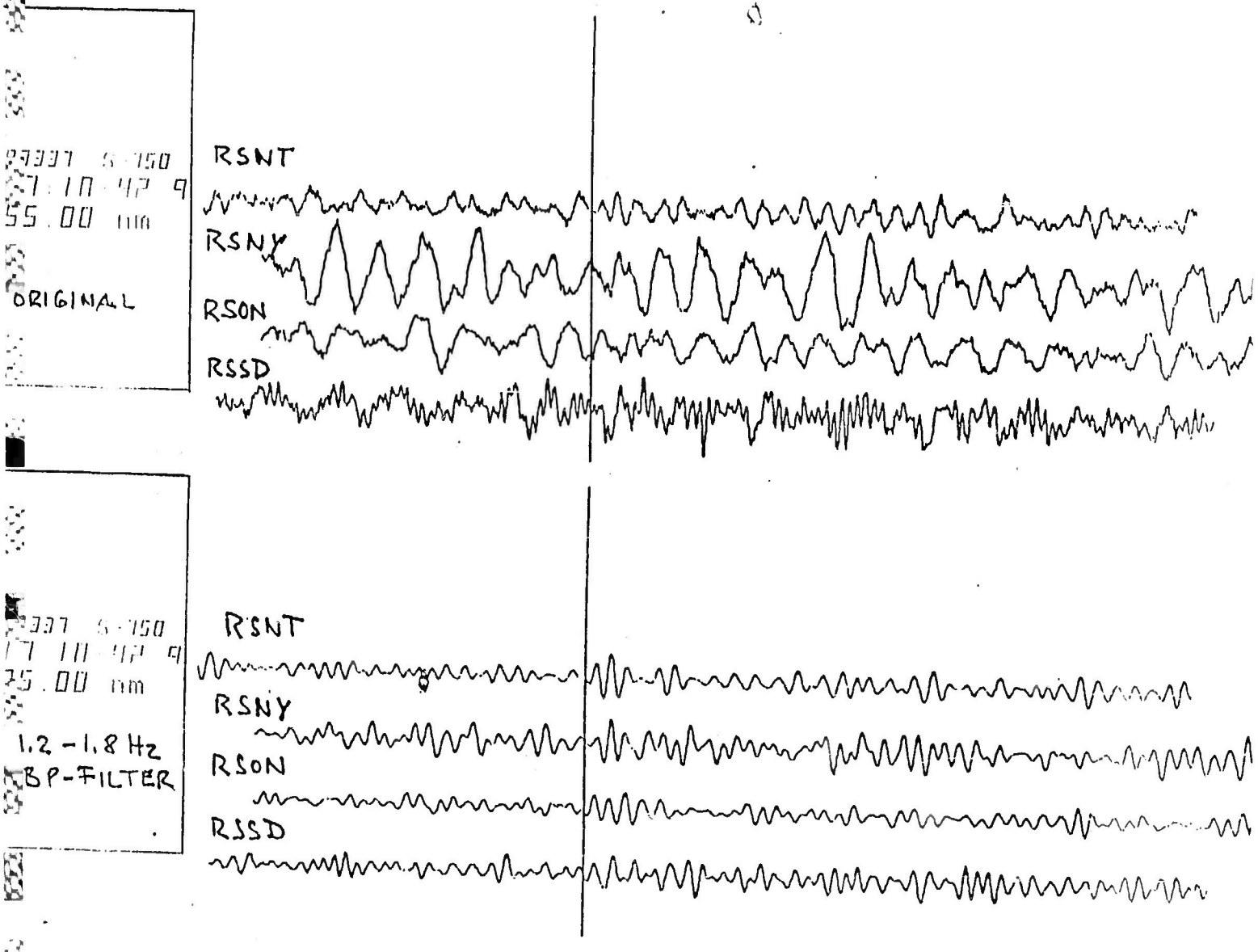

Fig 10: RSTN-recordings of French nuclear test (12/3/1983).
Upper traces are original data,
lower traces are bandpass-filtered.

```
EVENT 19 12/ 3/83 16:58: 3.5  -20.95 -139.87     9KM    6obs TUAMOTU ARCHIPELAGO REGION
        std. errors   ( 64.9) (145.6) (104.5) (393.3)     (in secs., Km.)

ALQ  17: 8:38.0 P      P        1   -1.4    64.0   6.5    30.2   214.9      3.4   0.9   4.0 -   4.3
CTA  17: 9: 8.0 P      P        1   -0.5    68.6   6.2   255.9   105.3      0.    0.    0. -
YKA  17:10:44.5        P        1    1.4    85.5   4.9    11.5   203.6     19.8   0.    0. -
                                             (beam)  5.0           206.6      3.8   0.8        4.6
GRF  17:17:36.1 PKPDF  PKPAB    1   -0.3   143.3   3.3    31.7   310.9      4.0   0.8   0. -   4.5
                                             (beam)  3.1           300.0
PRU  17:17:39.0 P      PKPDF    1    0.3   144.7   1.7    28.8   315.7      0.    0.    0. -
KHC  17:17:39.5 P      PKPDF    1    0.5   144.8   1.7    30.6   313.5      0.    0.    0. -
   mb=4.0 (+/-0.  ),on   1 obs
   Standard Error of observations =   2.6 on   6 of   6 observations
```

Fig 11 : Association result for French explosion using all WMO-messages at CSS.

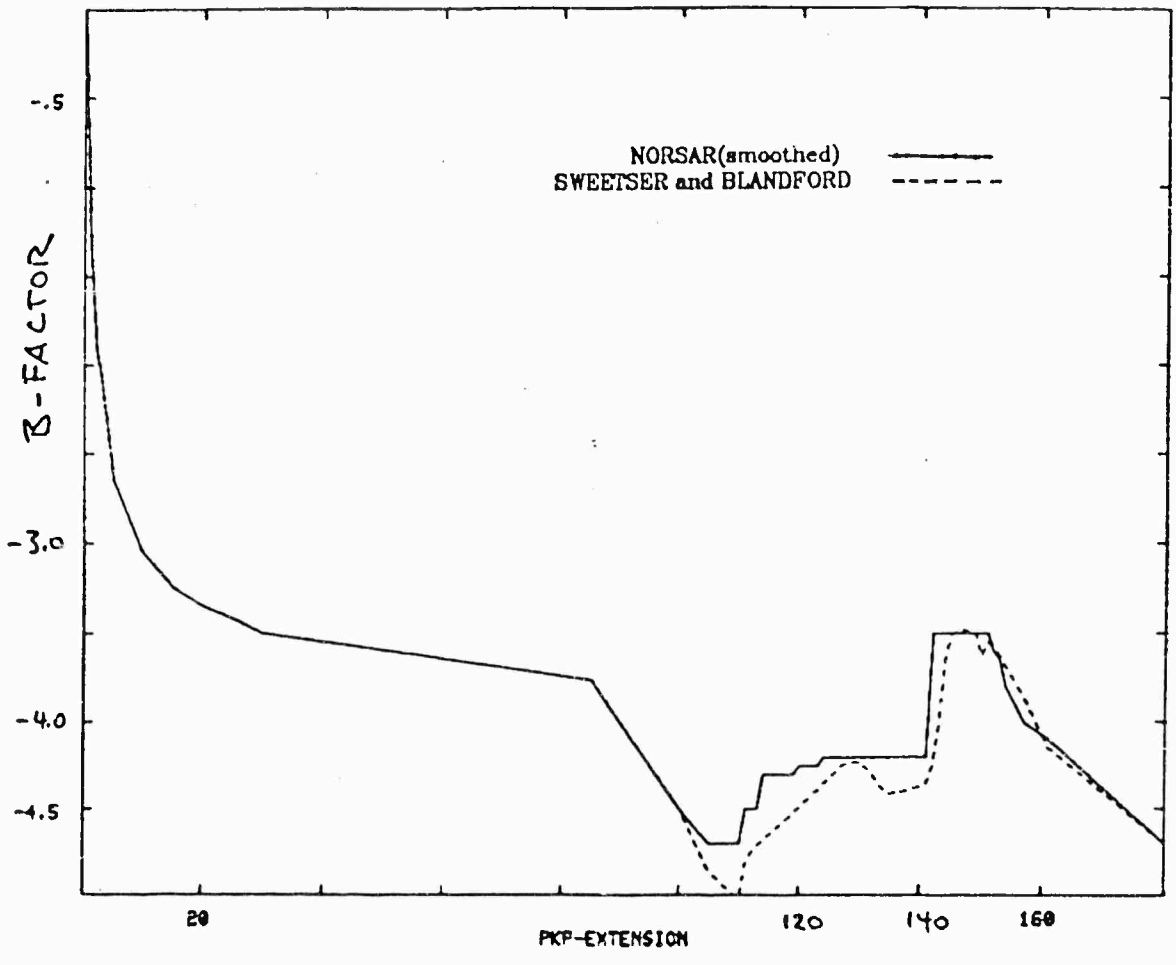
-.5
-3.0
-4.0
-4.5
B-FACTOR
NORSAR(smoothed)
SWEETSER and BLANDFORD
20
120
140
160
PKP-EXTENSION

Fig. 12

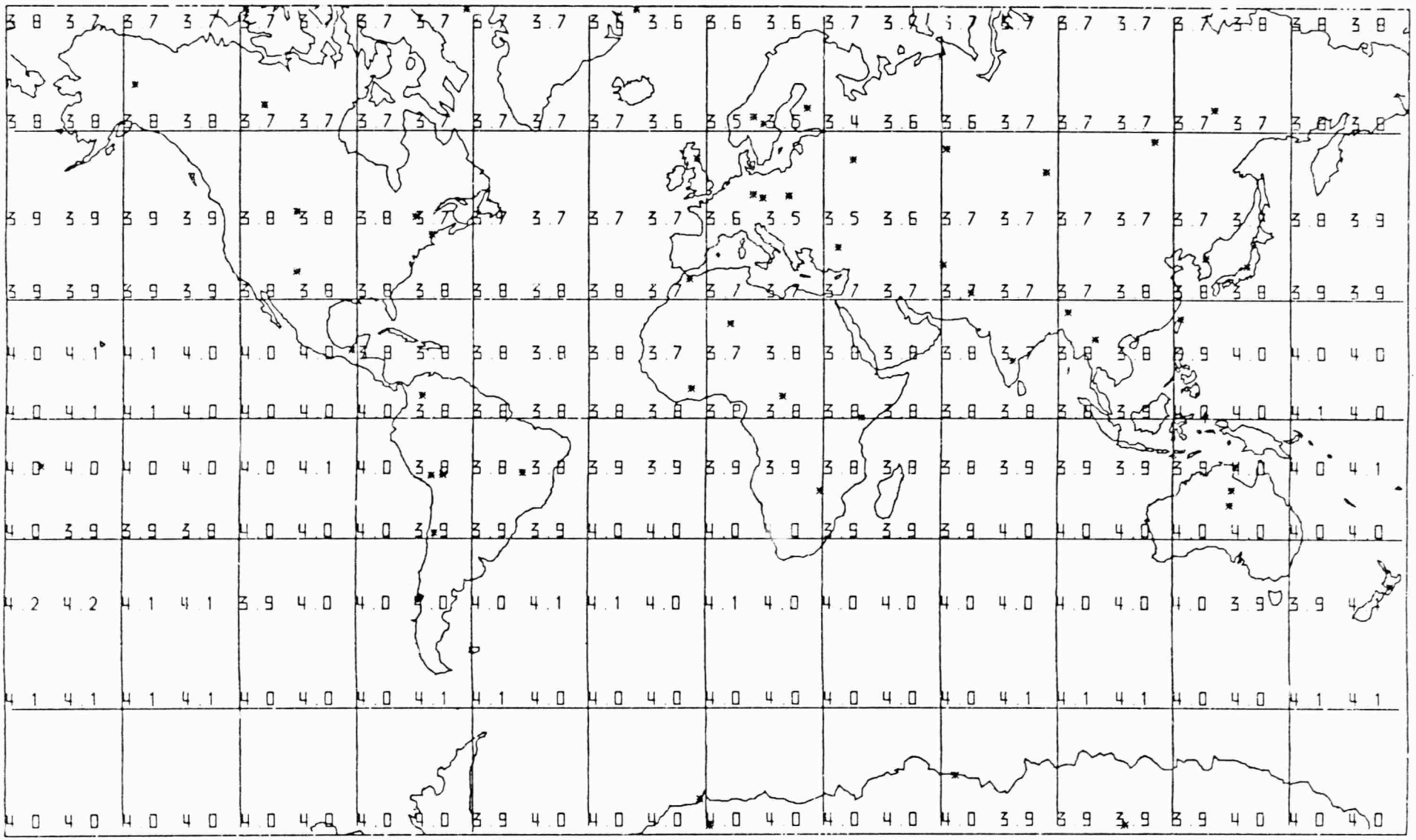

Fig 13:

(p+pkp)/4(at least p/1)-thresh.prob.=0.9 NORSAR-atten curve

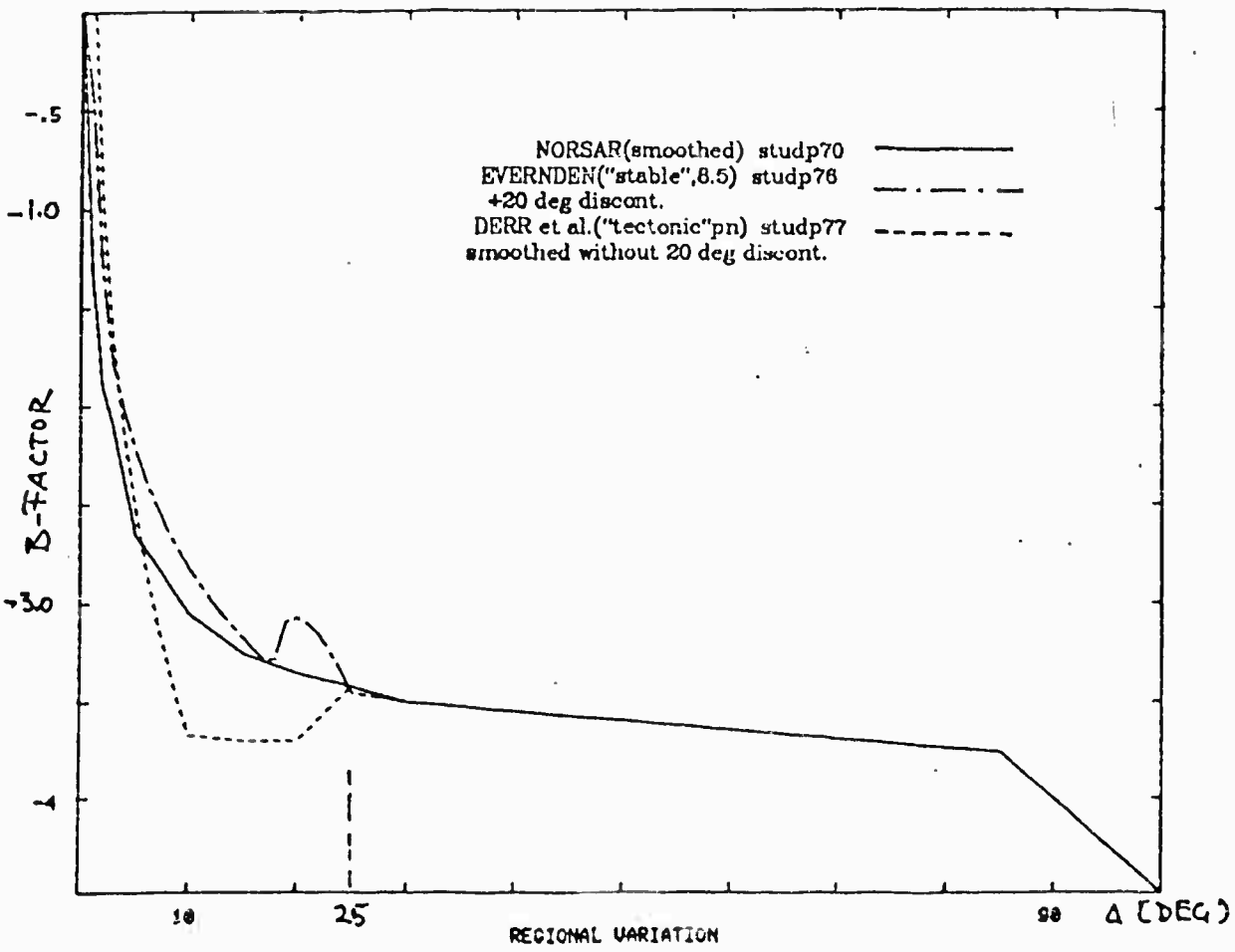
NORSAR(smoothed) studp70
EVERNDEN("stable",8.5) studp76
+20 deg discont.
DERR et al.("tectonic"pn) studp77
smoothed without 20 deg discont.
B-FACTOR
.5
1.0
1
10
25
90
Δ (DEG)
REGIONAL VARIATION

Fig 14:

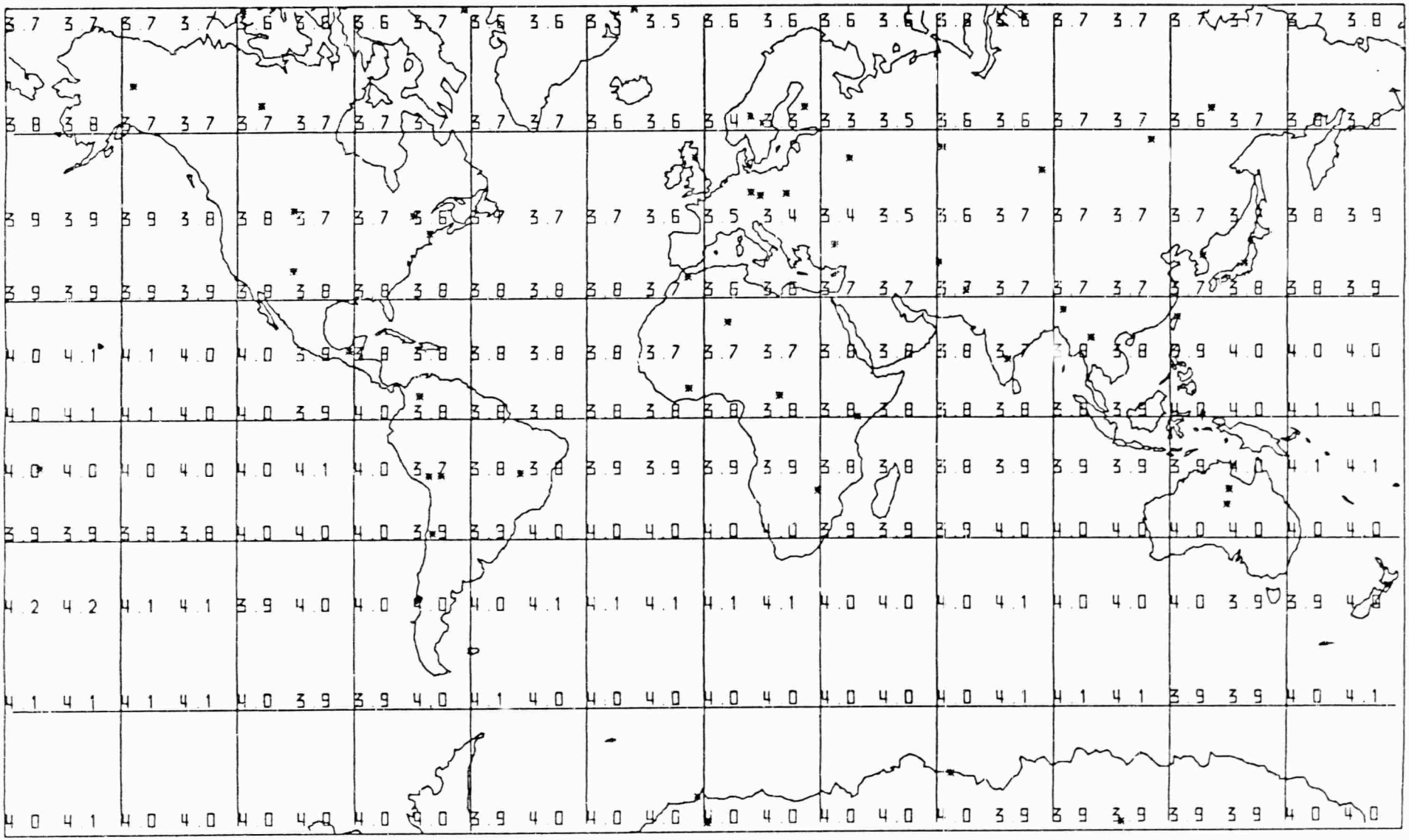

Fig 15: 50-station p/4-thresh prob =0.9 "stable" atten curve

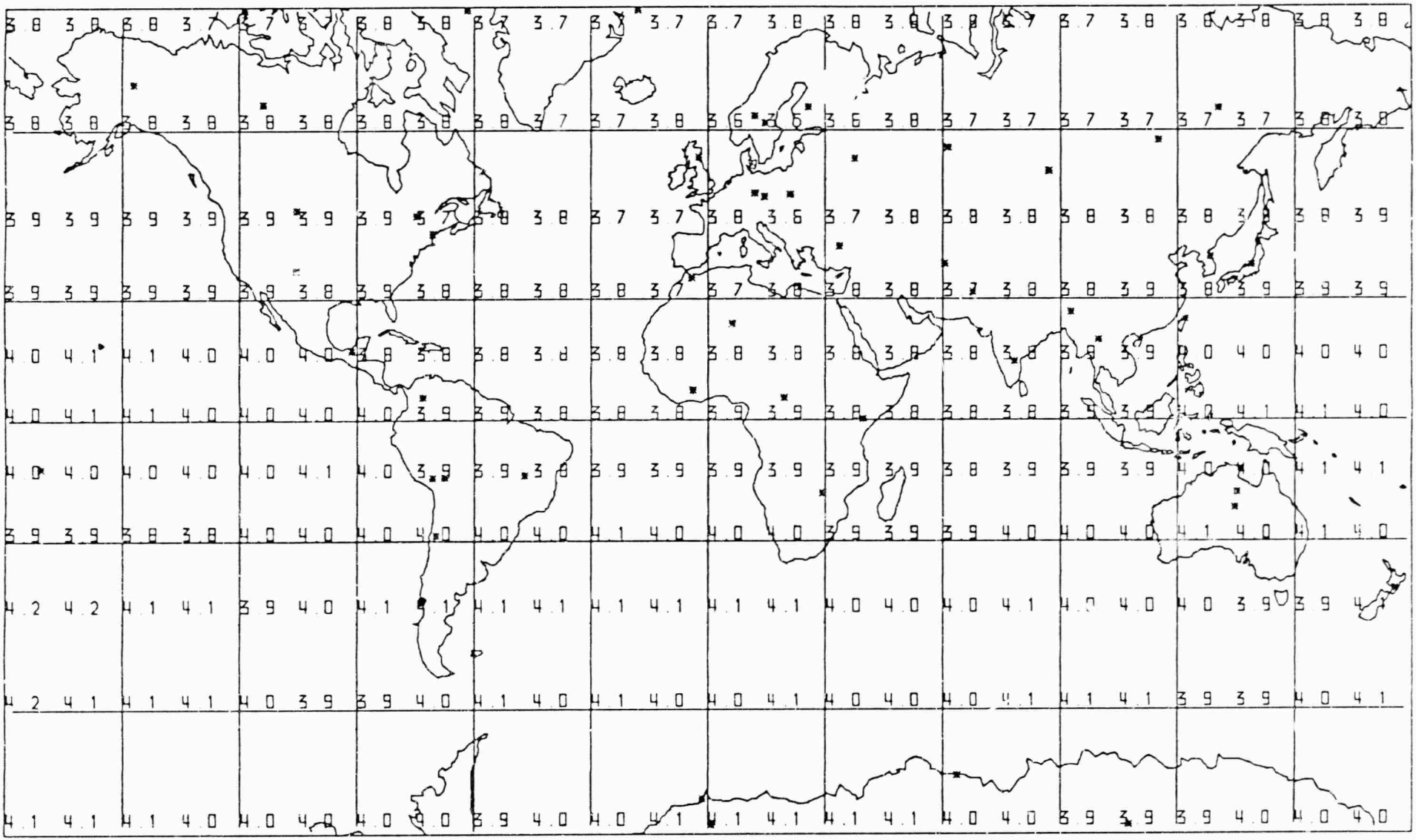

Fig.16: 50-station p/4-thresh prob =0.9 "tectonic" atten curve

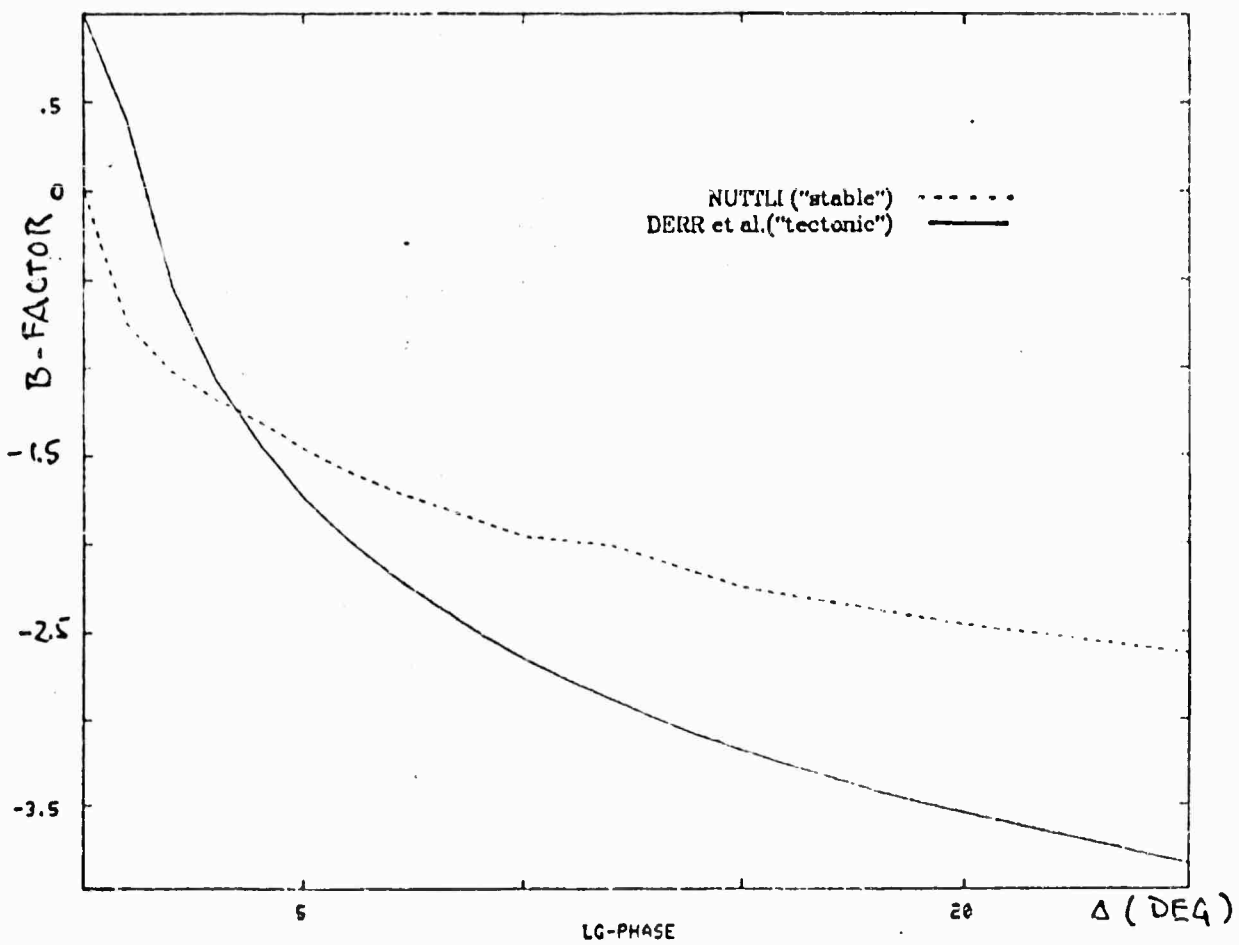
.5
0
-1.5
-2.5
-3.5
B-FACTOR
NUTTLI ("stable")
DERR et al.("tectonic")
5
20
LG-PHASE
Δ (DEG)

Fig. 17

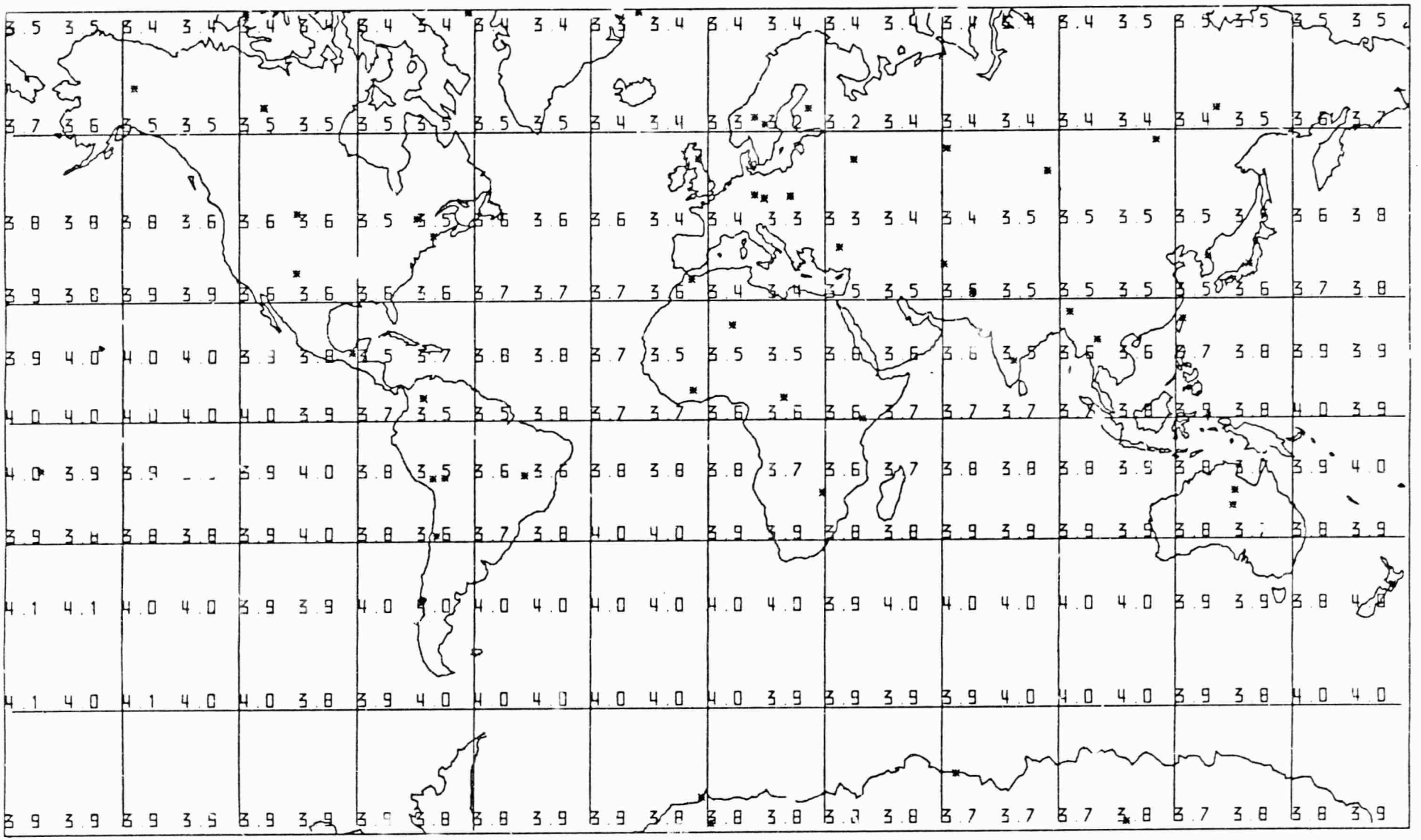

50-station (lg/2*p/1+p/4)-thresh prob =0.9 "stable" atten curves

Fig. 18

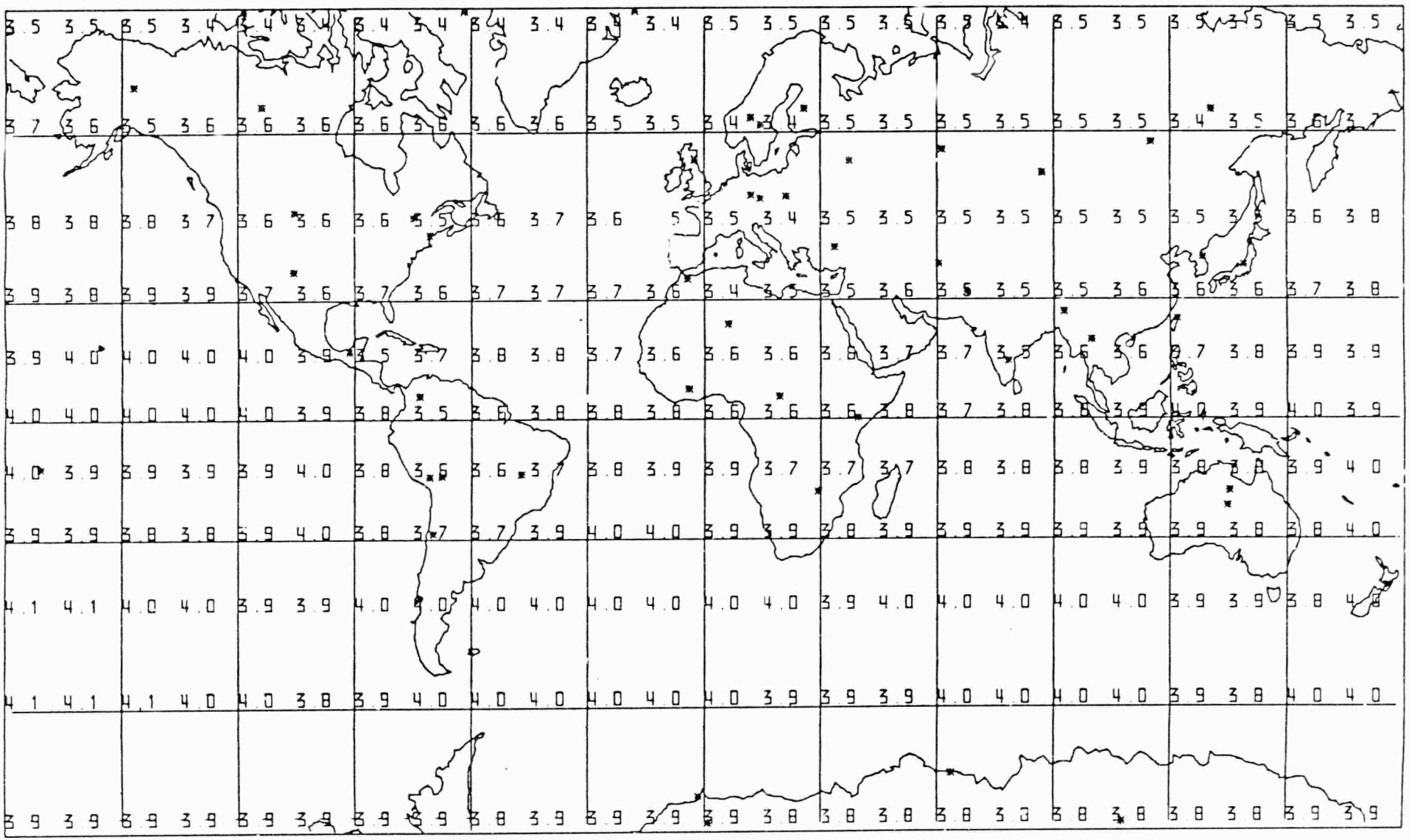

Fig 19: 50-station lg/2*p/1+p/4-thresh prob =0.9 "tectonic" atten curves

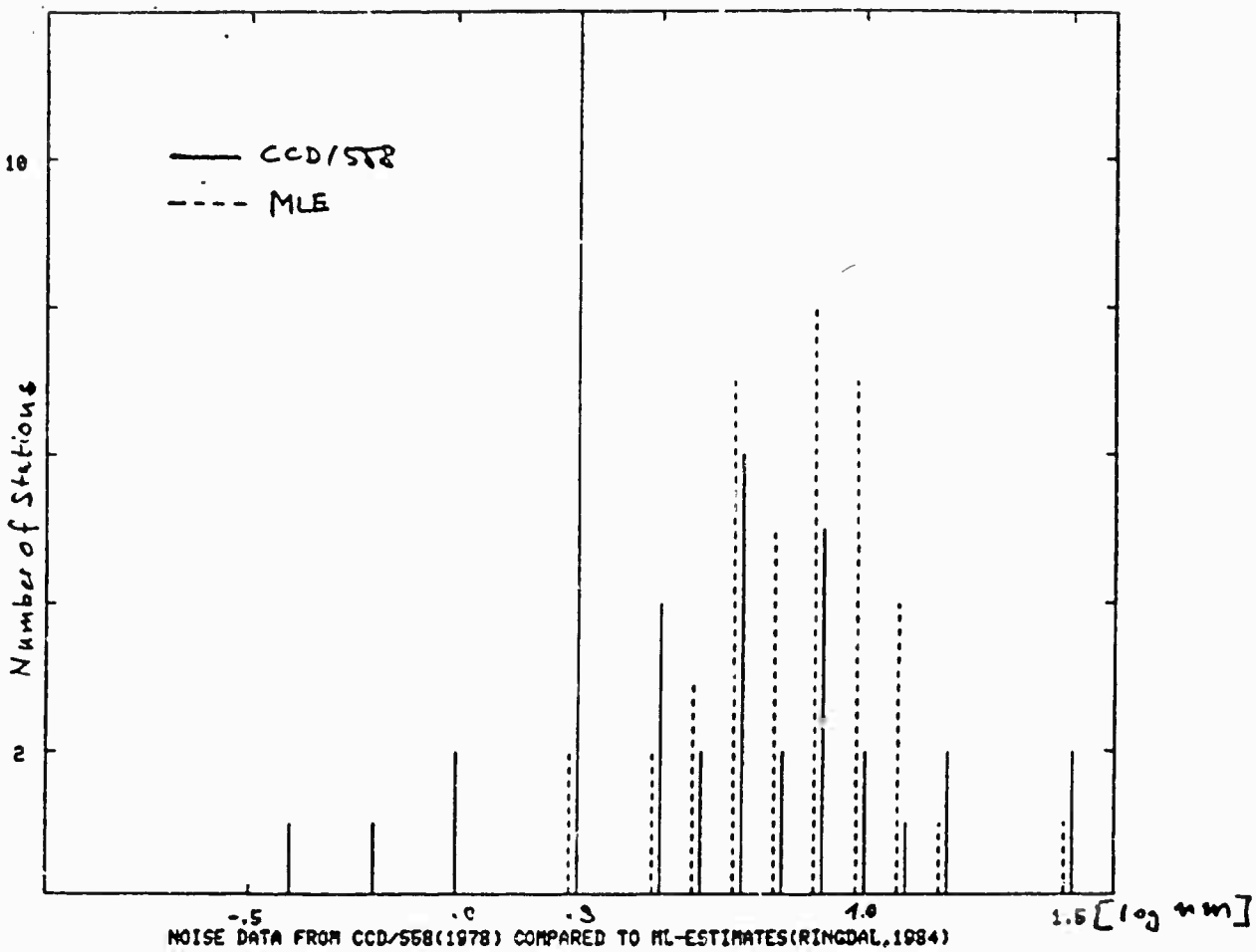
CCD/558
MLE
10
2
Number of Stations
-.5
.0
.5
1.0
1.5 [log mm]
NOISE DATA FROM CCD/558(1978) COMPARED TO ML-ESTIMATES(RINGDAL,1984)

Fig. 20

GRF A1Z Noise

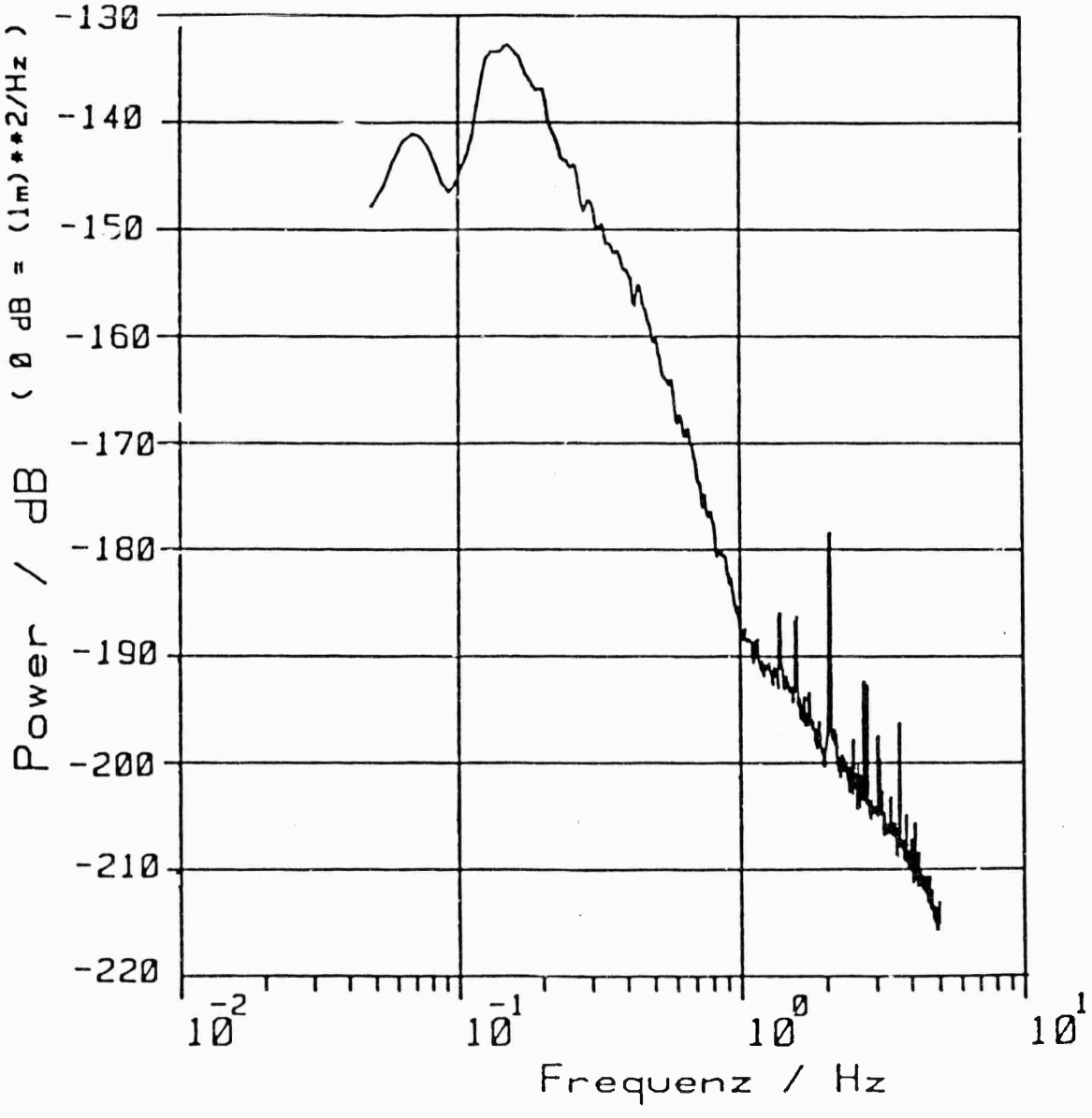

Fig. 21

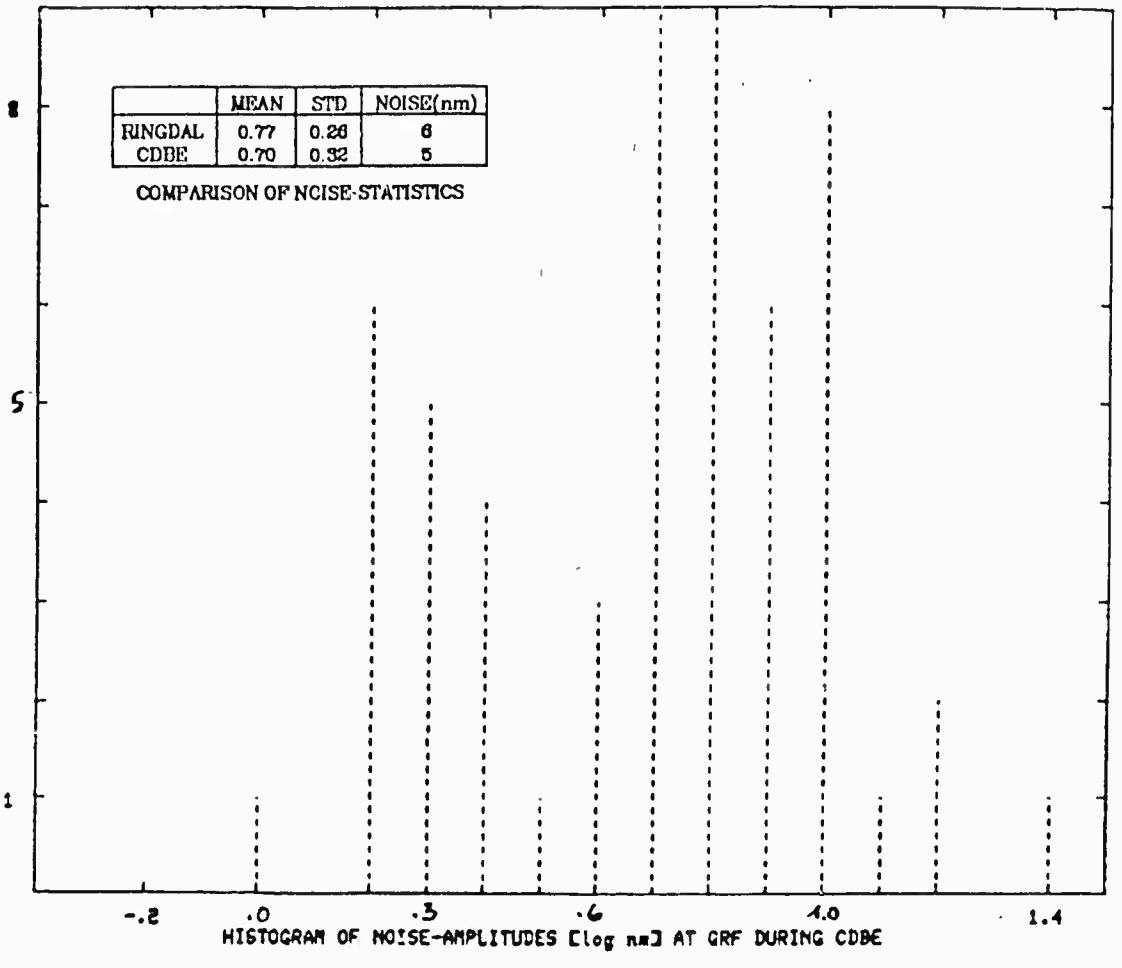
MEAN
STD
NOISE(nm)
RINGDAL
0.77
0.26
6
CDBE
0.70
0.32
5
COMPARISON OF NOISE-STATISTICS
8
5
1
-.2
.0
.3
.6
1.0
1.4
HISTOGRAM OF NOISE-AMPLITUDES [log nm] AT GRF DURING CDBE

Fig. 22

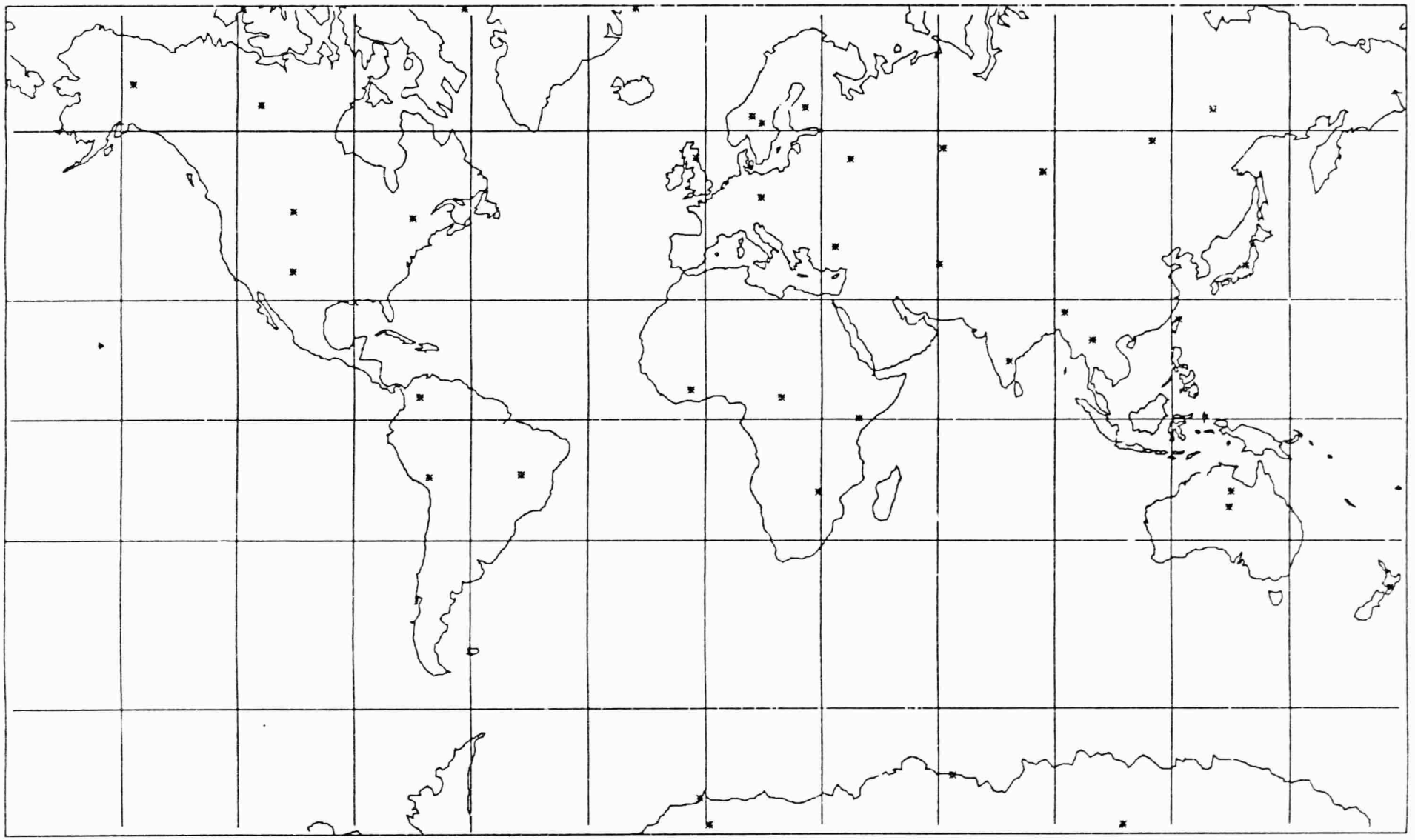

Fig.23: Global Seismic Network (39 stations from ISC-data(1980))

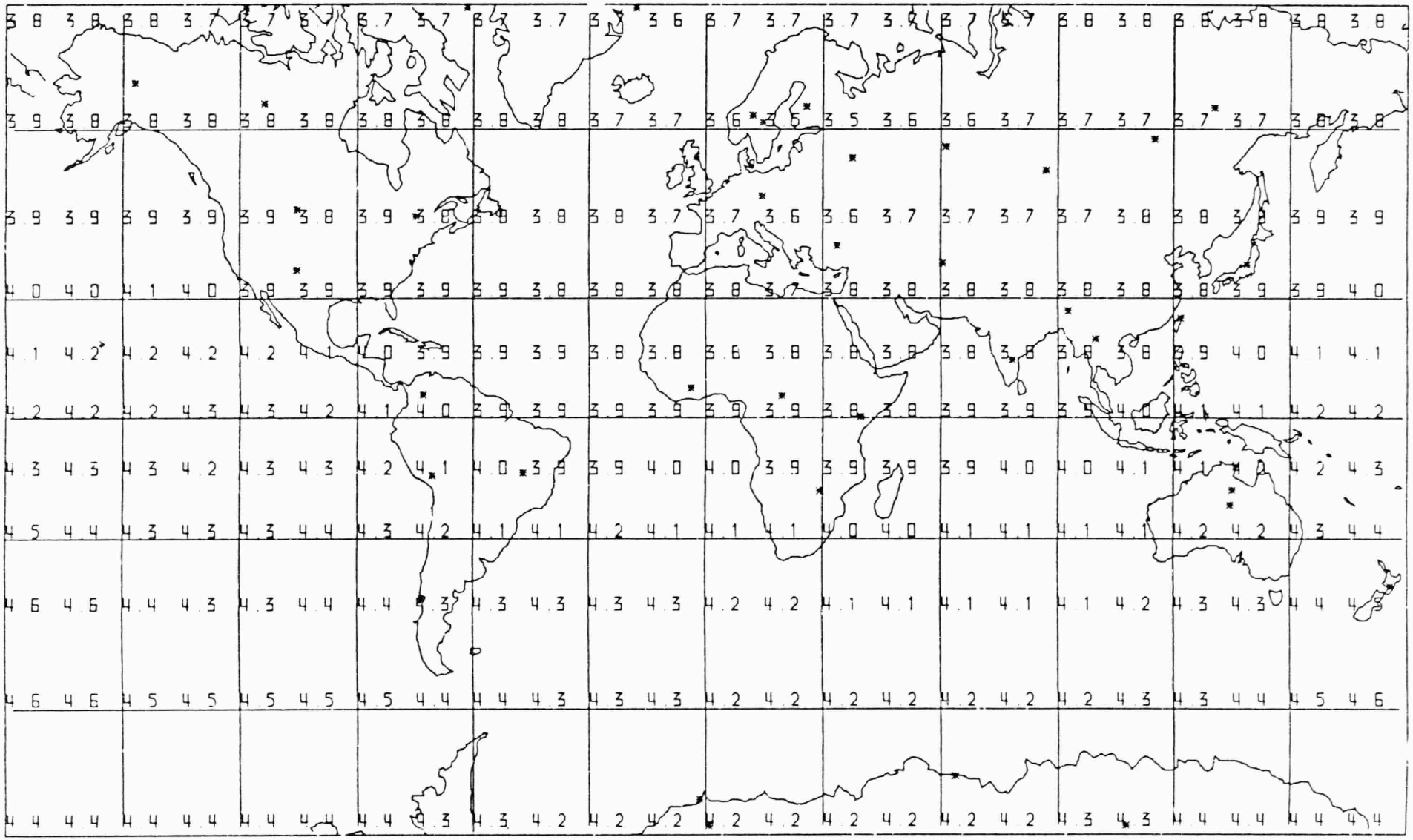

Fig.24: 39-station p/4-thresh prob =0 9 studp70 atten curve

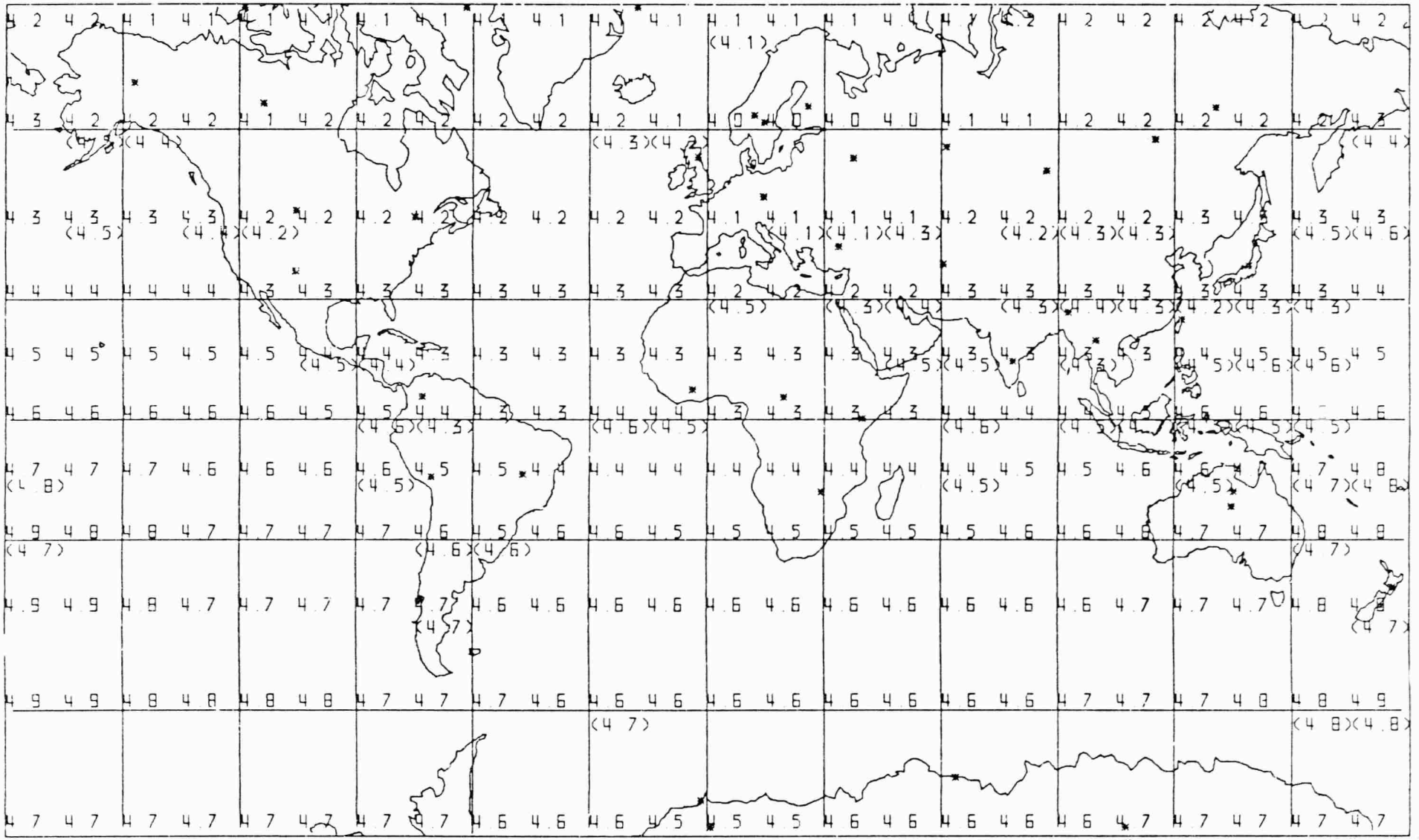

Fig 25: 39 ISC-station-p/4(p/1 teles)-det thresh prob =0.90